Graduate School ETD Form 9
(Revised 12/07)

PURDUE UNIVERSITY
GRADUATE SCHOOL
Thesis/Dissertation Acceptance

This is to certify that the thesis/dissertation prepared

By Nancy Giovanni Tanjung

Entitled
In Vitro and In Silico Analysis of Osteoclastogenesis in Response to Inhibition of De-phosphorylation of eIF2-alpha by Salubrinal and Guanabenz

For the degree of Master of Science in Biomedical Engineering

Is approved by the final examining committee:

Dr. Hiroki Yokota
Chair

Dr. Julie Ji

Dr. Sungsoo Na

To the best of my knowledge and as understood by the student in the *Research Integrity and Copyright Disclaimer (Graduate School Form 20)*, this thesis/dissertation adheres to the provisions of Purdue University's "Policy on Integrity in Research" and the use of copyrighted material.

Approved by Major Professor(s): Hiroki Yokota

Approved by: Edward J. Berbari 11/11/2013
Head of the Graduate Program Date

IN VITRO AND IN SILICO ANALYSIS OF OSTEOCLASTOGENESIS IN RESPONSE TO INHIBITION OF DE-PHOSPHORYLATION OF EIF2α BY SALUBRINAL AND GUANABENZ

A Thesis

Submitted to the Faculty

of

Purdue University

by

Nancy Giovanni Tanjung

In Partial Fulfillment of the

Requirements for the Degree

of

Master of Science in Biomedical Engineering

December 2013

Purdue University

Indianapolis, Indiana

ACKNOWLEDGMENTS

I would like to thank the Lord for the wisdom and perseverance that He has bestowed upon me during this thesis project and throughout my life: "I can do everything through Him who gives me strength." (Philippians 4:13).

I would like to express my profound gratitude and deep regards to my thesis advisor, Dr. Hiroki Yokota, for his excellent leadership, guidance, patience, and encouragement throughout the course of this thesis. Without him giving me the opportunity to do thesis research, I would not have gained the skills and knowledge I have right now. The written, verbal, research, and time management skills he taught me from time to time shall carry me a long way in the journey of life on which I am about to begin.

I would also like to express my sincere and deepest gratitude to Dr. Kazunori Hamamura, for his excellent and tremendous support and guidance throughout the thesis project. His patience, motivation, and immense knowledge have made it possible to get this project going and produce high quality data. It is such an honor to be taught by and work with a great scientist like him. My deepest gratitude also goes to Momoko Hamamura for her wonderful help and support throughout this thesis. Without her cheerful and kind personality, my days would not have been as bright as they were.

My sincere gratitude also goes to the rest of my committee members: Dr. Julie Ji and Dr. Sungsoo Na, for their encouragement, patience, and insightful comments. Without them, this thesis could not be completed.

I am grateful to have my co-worker, Andy Chen, to help and support me tremendously with math and programming. I am also thankful to have my friend, Mario Soliman, to always motivate and support me emotionally. They both have kept me from giving up and I am blessed to have them throughout the course of this thesis. I

would like to also thank my lab members and friends for supporting and encouraging me with their best wishes.

Finally, I would like to appreciate and thank my parents, my brother, and my host family for their unconditional support and prayers throughout my college career. Their patience, love, and understanding have motivated, encouraged, and kept me going. Without them and their support, I would not be able to reach the achievements that I have right now.

TABLE OF CONTENTS

Page

Page

LIST OF FIGURES

ABSTRACT

Tanjung, Nancy Giovanni. M.S.B.M.E, Purdue University, December 2013. In Vitro and In Silico Analysis of Osteoclastogenesis in Response to Inhibition of De-phosphorylation of EIF2α by Salubrinal and Guanabenz. Major Professor: Hiroki Yokota.

An excess of bone resorption over bone formation leads to osteoporosis, resulting in a reduction of bone mass and an increase in the risk of bone fracture. Anabolic and anti-resorptive drugs are currently available for treatment, however, none of these drugs are able to both promote osteoblastogenesis and reduce osteoclastogenesis. This thesis focused on the role of eukaryotic translation initiation factor 2 alpha (eIF2α), which regulates efficiency of translational initiation. The elevation of phosphorylated eIF2α was reported to stimulate osteoblastogenesis, but its effects on osteoclastogenesis have not been well understood. Using synthetic chemical agents such as salubrinal and guanabenz that are known to inhibit the de-phosphorylation of eIF2α the role of phosphorylation of eIF2α in osteoclastogenesis was investigated in this thesis.

The questions addressed herein were: Does the elevation of phosphorylated eIF2α (p-eIF2α) by salubrinal and guanabenz alter osteoclastogenesis? If so, what regulatory mechanism mediates the process? It was hypothesized that p-eIF2α could attenuate the development of osteoclast by regulating the transcription factor(s) amd microRNA(s) involved in osteoclastogenesis. To test this hypothesis, we conducted in vitro and in silico analysis of the responses of RAW 264.7 pre-osteoclast cells to salubrinal and guanabenz.

First, the in vitro results revealed that the elevated level of phosphorylated eIF2α inhibited the proliferation, differentiation, and maturation of RAW264.7 cells and downregulated the expression of NFATc1, a master transcription factor of osteoclastogenesis. Silencing eIF2α by RNA interference suppressed the downregulation of

NFATc1, suggesting the involvement of eIF2α in regulation of NFATc1. Second, the in silico results using genome-wide expression data and custom-made Matlab programs predicted a set of stimulatory and inhibitory regulator genes as well as microRNAs, which were potentially involved in the regulation of NFATc1. RNA interference experiments indicated that the genes such as Zfyve21 and Ddit4 were primary candidates as an inhibitor of NFATc1.

In summary, the results showed that the elevation of p-eIF2α by salubrinal and guanabenz leads to attenuation of osteoclastogenesis through the downregulation of NFATc1. The regulatory mechanism is mediated by eIF2α signaling, but other signaling pathways are likely to be involved. Together with the previous data showing the stimulatory role of p-eIF2α in osteoblastogenesis, the results herein suggest that eIF2αmediated signaling could provide a novel therapeutic target for treatment of osteoporosis by promoting bone formation and reducing bone resorption.

1. INTRODUCTION

1.1 Bone Remodeling

Bone is remodeled continuously during adulthood through the resorption of old bone by osteoclasts and the formation of new bone by osteoblasts. Osteoclasts are derived from hematopoietic stem cells while osteoblasts are derived from pluripotent mesenchymal stem cells. This bone remodeling event is important for renewing the skeleton while maintaining its anatomical and structural integrity. Under normal conditions, osteoclasts would adhere to bone and proceed to remove it by acidification and proteolytic digestion. Shortly after the osteoclasts leave the resorption site, osteoblasts would invade the area and begin the process of forming new bone by secreting osteoid, which is a matrix of collagen and other proteins, and eventually mineralize them [1, 2]. At the end of the bone remodeling process, the surface of the bone is covered by lining cells, which are a distinct type of terminally differentiated osteoblasts that control the microenvironment of the bone [3].

1.2 Background of Osteoporosis

Elevated bone resorption and reduced bone formation in the remodeling process leads to osteoporosis, where a reduction in bone mass, quality, and strength occurs resulting in an increased susceptibility to bone fractures [4]. Both men and women experience osteoporosis, primarily as a consequence of the aging process and the loss of gonadal function, but it is commonly diagnosed in postmenopausal women [5, 6]. Beginning around the fourth or fifth decade of life, both men and women lose bone at a rate of 0.3 to 0.5 percent per year. After menopause, the rate of bone loss

can increase as much as 10-fold [7–10]. Osteoporosis causes more than 8.9 million fractures annually and is estimated to affect 200 million women worldwide, of which 80% are women aged 60 years or older [11, 12]. Blume et. al. estimated that the US medical costs for osteoporosis range from $10 to $22 billion each year. In addition to the financial burden, osteoporosis and osteoporotic fractures are also associated with sustained disability, physical limitations, psychosocial impairment, and reduced quality of life [13].

Many factors could lead to the development of osteoporosis, including mineral deficiencies, hormone deficiencies, and long term disuse or the lack of activity. However, it is mainly caused by the aging process and more commonly experienced by women than men due to the drastic decrease in estrogen level during and after menopause [4]. Bone loss as a result of aging is associated with a progressive decline in the supply of osteoblasts in proportion to the demand of them. The demand, in this case, is determined by the frequency in which new multicellular units are created and new cycles of remodeling are initiated [14–16]. Estrogens are the primary female hormones produced by the ovaries and have an important role in maintaining the appropriate ratio of osteoblasts and osteoclasts [17]. When the estrogen level is reduced, the osteoclast activity is increased, resulting in longer bone resorption periods [18]. Bone loss caused by aging and menopause not only differ in the underlying cellular changes but also in the affected skeletal locations. Aging-related bone loss occurs primarily in cortical bone while postmenopausal bone loss occurs primarily in trabecular bone [1].

1.3 Current Available Treatment and Side Effects

In the past 20 years, many therapeutic treatments have been developed to prevent osteoporosis, yet cost, efficiency, and side effects are still the issues needed to be tackled. Most of these treatments involve the administration of drug supplements, dietary changes, and prevention of falls or impacts to avoid fractures. Although they might show promise in reducing the harmful effects of osteoporosis, there are many

disadvantages due to the adverse side effects. Calcium and vitamin D supplements have shown some success in clinical studies to raise the calcium content in the bone and help to inhibit osteoclast precursors [19–22]. However, a study in 2012 by Moyer et al. said the effects of calcium and vitamin D supplements seemed to be limited for the patients who already show symptoms of osteoporosis [23]. Another study also showed a linkage between the use of calcium supplements and an increased risk of cardiovascular disease and heart attack [22, 24]. Hormone replacement therapies have also been used to prevent osteoporotic fractures and reduction in bone mass in post-menopausal women. However, an increased risk of breast cancers has been reported as a side effect for long-term hormone replacement therapies [25, 26].

Human hormones and antibodies have also been used to prevent and treat osteoporosis. Parathyroid hormone (PTH) has been given to osteoporosis patients as a daily injection and was proven to be able to stimulate pre-osteoblasts to mature into bone-forming osteoblasts which would lay down collagen and mineralize matrix [27]. However, since the bone formation is always coupled with bone resorption, once pre-osteoblasts are stimulated, they release cytokines that can also activate osteoclasts activity. Therefore, in the long term, this treatment could lead to a re-equilibration such that resorption catches up to formation of bone. Since PTH therapy has the potential risk of carcinogenicity, the treatment is limited to those most severely affected and for a maximum of two years [28, 29]. Denosumab, an FDA-approved antibody, is an antiresorptive agent due to its property that inhibits the activation of osteoclasts by mimicking the action of osteoprotegerin (OPG), a decoy receptor for receptor activator of nuclear factor kappa-B ligand (RANKL) [30, 31]. RANKL is a cytokine belonging to the tumor necrosis family found in osteoblasts and involved in T cell-dependent immune responses as well as differentiation and activation of osteoclasts [32, 33]. Denosumab is administered subcutaneously only twice a year and the effect is potentially reversible. However, the immune system might be affected, and the long term effect is still unknown [34]. All agents that are given parenterally require professional training and aseptic technique to administer those [35].

Synthetic drugs are taken orally and could be made to give the same bioavailability as parenteral drugs. The cost is usually cheaper and does not require any professional training. The most widely prescribed synthetic drugs to treat post-menopausal osteoporosis are bisphosphonates. Bisphosphonates inhibit osteoclast progenitor development and promote osteoclast apoptosis while preventing osteocyte and osteoblast apoptosis [36]. Although this mechanism seems appealing, there are some significant side effects accompanying the benefits. Bisphosphonates have been associated with an increased risk of osteonecrosis of the jawbone, which is indicated by the exposure and death of bone tissue through lesions in the mouth [37, 38]. Another concern would be that micro-damage may start appearing in the bone and eventually lead to fracture since bisphosphonates alter the bone remodeling cycle [39]. Since the currently available therapeutic drugs are still inadequate, a new effective treatment for osteoporosis is needed.

1.4 Effects of eIF2α Phosphorylation

eIF2α signaling plays a key role in determining cell fate, especially under stress conditions, due to its ability to promote either cellular recovery and pro-survival pathways or apoptosis. eIF2α has been known to be phosphorylated in response to different stressful conditions which potentially lead to cellular apoptosis in cells such as viral infection, nutrient deprivation, oxidation, and stress in the endoplasmic reticulum [40–42]. Phosphorylation of eIF2α reduces global protein translation and shifts the translation machinery to favor the translation initiation of some selective stress response genes, including activating transcription factor 4 (ATF4). This transient attenuation of protein synthesis is believed to reduce the load of substrates presented to the folding machinery in the ER lumen during stress and giving time for the chaperones, proteases, and stress responsive genes to try recovering the cells [42].

How exactly eIF2α chooses the cellular fate in the presence of stress is complicated and not well understood. When eIF2α phosphorylation is induced by mild

stresses, the stress could be alleviated by the activation of pro-survival signaling [43]. However, in response to severe prolonged stress, the phosphorylation of eIF2α would lead to the apoptosis pathway [44]. Both pro-survival and apoptosis signaling might vary between cell types and between eIF2α phosphorylation inducers (stress or compounds). In most cases, part of the decision has been reported to be mediated by C/EBP homologous protein (CHOP). The phosphorylation of eIF2α is known to upregulate the translation of ATF4, which activates the expression of CHOP. Therefore, CHOP expression is stringently dependent upon eIF2α phosphorylation [45]. CHOP upregulates GADD34 and ER oxidase 1α (ERO1α) which restores the activity of general protein synthesis through the de-phosphorylation of eIF2α and enhances protein folding in the ER, respectively. CHOP also stimulates the production of reactive oxygen species which induce oxidative stress that, when too strong, would lead to cell death [46]. A study on mouse embryonic fibroblasts cells identified some downstream of CHOP (DOC) genes such as DOC4, which has signaling properties that effect the process of regeneration of cells, and DOC 6, which contributes to the development of programmed cell death [45]. This ability of CHOP to promote cellular recovery or cell death indicates that there is a fine balance in the cell condition to determine the outcome of adaptation to and alleviation of stress [47]. This balance might depend on the level of cellular stress, the cell types, and the cellular context; however, the key still lies with the regulation of eIF2αdependent translation which is important in modulating ER protein folding load and in managing stress [48].

1.5 Salubrinal and Guanabenz as Inhibitors of eIF2α Dephosphorylation

Salubrinal was first discovered for its cytoprotective and anti-apoptotic effects on rat pheochromocytoma PC12 cells exposed to a cytotoxic environment and apoptotic stimulus specific for endoplasmic reticulum stress (ER stress). When the mechanism on how salubrinal protects the cells from ER stress was further investigated, it was found that salubrinal induced rapid and robust eukaryotic initiation factor 2 subunit

alpha (eIF2α) phosphorylation. Salubrinal is distinct from ER stress inducers like Tunicamycin, in that salubrinal phosphorylation of eIF2α does not depend on any single known eIF2α kinase such as PERK, GCN2, PKR, and HRI, and does not cause any disturbance or stress to the cells [49]. Instead, it was found to inhibit the de-phosphorylation of eIF2α by interacting with protein phosphatase 1 (PP1) and prevent it from forming a dimer with growth arrest and DNA damage (GADD) 34, a mechanism that is not found in any chemicals that induce the phosphorylation of eIF2α [40, 49].

Through changing the phosphorylated level of eIF2α salubrinal may induce a stimulatory or inhibitory effect depending on administration conditions such as dose, as well as cell types and physiological states. For example, it was reported that salubrinal suppressed tunicamycin-induced cardiomyocyte apoptosis [50]. Salubrinal's pro-survival effects were also reported in human bronchial epithelial cells in response to cigarette smoke extract, and human neuroblastoma cells to ceramide [51, 52]. On the other hand, the responses to salubrinal apparently differ when it was administered to cancer cells. For instance, salubrinal stimulated the pro-apoptotic pathway in leukemic cells [53] and increased radiation-induced cell death in chondrosarcoma cells [54]. Moreover, it suppressed the survival and growth of multiple myeloma cells, head and neck carcinoma cells, and breast cancer cells [55–57].

Another synthetic agent, guanabenz acetate (guanabenz), utilizes a mechanism of action similar to that of salubrinal. Guanabenz is an FDA-approved drug currently used to treat patients with high blood pressure. The structure of guanabenz is smaller than salubrinal, and when immersed in an acidic environment, it breaks down into 2,6-dichlorobenzaldehyde and aminoguanidine [58]. It was reported that guanabenz is also capable of selectively inhibiting GADD34-mediated dephosphorylation of eIF2a through interacting with PP1 and GADD34 dimer. Guanabenz was shown to exert a cytoprotective effect against ER stress by prolonging eIF2α phosphorylation and translation attenuation in HeLa cells [41]. Guanabenz was also shown to protect photoreceptors from retinal degeneration, which was caused by abnormal protein

retention in the ER [59]. Both salubrinal and guanabenz have been used as selective inhibitors of eIF2α dephosphorylation, and the effects of eIF2αmediated signaling in ER-stress related diseases have been investigated using various cells and tissues.

1.6 Elevation of eIF2α Phosphorylation by Salubrinal and Guanabenz in Bone Cells

Previous studies indicate that there is a close association of ER stress with osteoporosis. To our knowledge, however, no therapeutic agents for osteoporosis have been targeted to eIF2αmediated signaling. Stress in the ER could be caused by aging, genetic mutations, diet, or environmental factors, which include some of the factors influencing osteoporosis. A study in 2010 correlated the pathogenesis of osteoporosis with ER stress response in the osteoblasts of osteoporosis patients. This study found that ER molecular chaperones, such as BiP (immunoglobulin heavy-chain binding protein) and PDI (protein-disulfide isomerase) are downregulated in osteoblasts from osteoporosis patients [60]. Another study showed that ER stress sensor PERK (protein kinase-like ER kinase) is associated with lowered bone mineral density (BMD) and abnormal compact bone development [61].

The observed phenotypes of PERK-deficient mice are very similar to those of ATF4-deficient mice. As mentioned before, eIF2α phosphorylation induces the expression of ATF4 which is known to be the key transcription factor for osteoblast terminal differentiation and bone formation. Mice that are ATF4-deficient exhibit a marked reduction or delay in the mineralization of bones [62]. Analyses on bone tissues revealed that PERK-deficient mice show severe osteopenia caused by a deficiency in the number of mature osteoblasts and impaired osteoblast differentiation [63]. Interestingly, ER stress was reported to be involved during osteoblasts differentiation induced by bone morphogenic protein 2 (BMP2) in culture through the PERK-eIF2α-ATF4 signaling pathway, which was then followed by the promotion of osteogenic genes such as osteocalcin (OCN) and bone sialoprotein (BSP) [64].

A separate study in our research group revealed that the elevation of p-eIF2α by salubrinal and guanabenz stimulates development of osteoblasts. This study showed that in osteoblasts, elevation of phosphorylated eIF2α by salubrinal and guanabenz enhances mineralization, stimulates expression of ATF4, and promotes osteoblast differentiation in vitro [65, 66]. Using a rat animal model, the subcutaneous injection of salubrinal showed accelerated closure of surgically generated bone wounds by modifying the expression of stress-sensitive genes [67]. Administration of salubrinal also promotes osteoblast differentiation in bone marrow-derived cells taken from ovariectomized (OVX) mice, an animal model that exhibits osteoporosis-like symptoms due to the drastic decrease in estrogen [68]. Taken together, salubrinal and guanabenz could enhance osteoblast development and promote bone formation through the elevation of phosphorylated eIF2α .

Since the elevation of phosphorylated eIF2α was shown to have a positive effect on the development of osteoblasts, its effect on the development of osteoclasts needs to be investigated. Osteoblasts and osteoclasts extensively interact through molecular pathways including RANK/RANKL/OPG and Wnt signaling [69]. Therefore, osteoclastogenesis is potentially regulated by signaling molecules that also affect osteoblastogenesis. Furthermore, osteoclastogenesis is influenced by various stresses such as estrogen deficiency and disuse or unloading [64]. However, eIF2αmediated signaling on bone resorption has not been well understood, particularly its role in the development of osteoclasts.

1.7 Questions, Hypothesis, and Approach

The goal of this thesis was to investigate the effect of the inhibition of eIF2α dephosphorylation by salubrinal and guanabenz on the development of osteoclasts. The questions addressed were: Does the elevation of p-eIF2α by salubrinal and guanabenz alter osteoclastogenesis? If so, what regulatory mechanism mediates the process? The elevation of p-eIF2α suppresses the global translation efficiency and induces tran-

scription regulation on cellular development. Thus, It was hypothesized that p-eIF2α attenuates the development of osteoclast by regulating the transcription factor(s) and microRNA(s) involved in osteoclastogenesis.

To test this hypothesis, we administered salubrinal and guanabenz to RAW 264.7 pre-osteoclasts cells. Using an in vitro approach, we determined the mRNA and protein levels of regulatory molecules involved in osteoclastogenesis, including NFATc1 that is the key transcription factor of osteoclast development. This in vitro approach includes TRAP staining, quantitative PCR for mRNAs and microRNAs (miRNAs), western blot, and gene silencing by RNA interference. MicroRNAs are a class of small non-coding regulatory RNAs that regulate mRNA expression. The binding of miRNAs to the 3'-untranslated region (UTR) of their target mRNAs is considered to reduce expression of mRNAs [70]. A genome-wide microarray analysis was conducted to determine the expression levels of mRNAs and microRNAs. Through in silico approaches with custom-made Matlab programs, we predicted stimulatory and inhibitory genes as well as microRNAs that were potentially involved in the regulation of NFATc1. Furthermore, we predicted microRNAs that potentially regulate the regulatory gene candidates. RNA interference was used to evaluate in silico predictions.

2. MATERIALS AND METHODS

2.1 *In Vitro* Analysis

2.1.1 Cell Culture

RAW 264.7 mouse pre-osteoclast (monocyte/macrophage) cells were cultured in α-MEM media containing 10% fetal bovine serum and antibiotics (50 units/ml penicillin and 50 µg/ml streptomycin; Life Technologies, Grand Island, NY, USA). Cells were grown in culture dishes and maintained in a humidified incubator at 37℃ containing 5% CO_2.

2.1.2 TRAP Staining

The effect from different doses of salubrinal and guanabenz on osteoclastogenesis was observed using TRAP staining. The RAW264.7 cells were plated at a density of $5 \times 10^3/cm^2$ into a 12-well plate or a 60 mm dish, and cultured with 20 ng/ml RANKL in the presence and absence of 0.1–20 µM Salubrinal or 1–20 µM Guanabenz acetate (Tocris Bioscience, Ellisville, MO, USA). The culture medium was replaced every 2 days. After 5 days of culture, the cells were stained for TRAP using an acid phosphatase leukocyte kit (Sigma, St. Louis, MO, USA). The number of TRAP-positive cells containing three or more nuclei was determined.

2.1.3 Quantitative Real-time PCR

To obtain the mRNA levels of genes involved in osteoclastogenesis, quantitative real-time polymerase chain reaction (PCR) was used. Total RNA was extracted using an RNeasy Plus mini kit (Qiagen, Germantown, MD, USA). Reverse transcription was conducted with high capacity cDNA reverse transcription kits (Applied Biosystems, Carlsbad, CA, USA), and quantitative real-time PCR was performed using ABI 7500 with Power SYBR green PCR master mix kits (Applied Biosystems). We evaluated the mRNA levels with the PCR primers listed in Figure 2.1. GAPDH was used for internal control. The relative mRNA abundance for the selected genes with respect to the level of GAPDH mRNA was expressed as a ratio of $S_{\text{treated}}/S_{\text{control}}$, where S_{treated} was the mRNA level for the cells treated with chemical agents, and S_{control} was the mRNA level for control cells.

2.1.4 Western Immunoblotting

To quantify the protein levels of different genes involved in osteoclastogenesis, Western immunoblotting was conducted. Cells were lysed in a radioimmunoprecipitation assay (RIPA) buffer containing protease inhibitors (Santa Cruz Biotechnology, Santa Cruz, CA, USA) and phosphatase inhibitors (Calbiochem, Billerica, MA, USA). Isolated proteins were fractionated using 10-15% SDS gels (BioRad, Hercules, CA, USA) and electro-transferred to Immobilon-P membranes (Millipore, Billerica, MA, USA). Membranes were incubated for 1 hour with primary antibodies followed by a 45-minute incubation with goat anti-rabbit or anti-mouse IgG conjugated with horseradish peroxidase (Cell Signaling, Danvers, MA, USA). We used antibodies against NFATc1 (Santa Cruz), p-eIF2α (Thermo Scientific, Waltham, MA, USA), eIF2α p38 and p-p38 mitogen activated protein kinase (MAPK), extracellular signal-regulated kinase (ERK) and p-ERK, nuclear factor kappa B (NFκB) p65 and p-NFκB p65 (Cell Signaling), and β-actin (Sigma, St. Louis, MO, USA). Protein levels were assayed using a SuperSignal west femto maximum sensitivity substrate (Thermo Sci-

Fig. 2.1. Real-time PCR primers used

Gene	Forward Primer	Reverse Primer
NFATc1	5'- GGTGCTGTCTGGCCATAACT -3'	5'- GCGGAAAGGTGGTATCTCAA -3'
c-Fos	5'- AGGCCCAGTGGCTCAGAGA -3'	5'- CCAGTCTGCTGCATAGAAGGAA -3'
TRAP	5'- TCCTGGCTCAAAAAGCAGTT -3'	5'- ACATAGCCCACACCGTTCTC -3'
OSCAR	5'- ACACACACACCTGGCACCTA -3'	5'- GAGACCATCAAAGGCAGAGC -3'
Dscr1	5'- CCCGACAAACAGTTCCTCAT -3'	5'- CACACTGGGAGTGGTGTCTG -3'
Dusp2	5'- TGGAAATCTTGCCCTACCTG -3'	5'- CTCCTGGAACCAGGCACTTA -3'
Jdp2	5'- CTTCCCAGCTCTGCTCTGAC -3'	5'- GCCTTTTCCTTCGCTCTTCT -3'
Adora2b	5'- GCGAATAAAAGCTGCTGTCC -3'	5'- CCTGGAGTGGTCCATCAGTT -3'
Ptpn22	5'- ATAGCAACCCACACGACTCC -3'	5'- TGCTCCAAATGTTACCACCA -3'
Syt16	5'- GGAGACGGAGACAGCTTTTG -3'	5'- GTTGACACCACTTCGGTCCT -3'
Nfkb1	5'- CTGACCTGAGCCTTCTGGAC -3'	5'- GCAGGCTATTGCTCATCACA -3'
Lats1	5'- AAAGACGTTCTGCTCCGAAA -3'	5'- TTCAGGAAAGATGCCCATTC -3'
Hipk2	5'- CTTCCAGCACAAGAACCACA -3'	5'- ACCTTCACTCGGTACGGTTG -3'
Traf1	5'- CTGGCGGTCTTAAAGGAGTG -3'	5'- AAACACACGCAGCTTCTCCT -3'
Bcl3	5'- GGACCTTTGATGCCCATTTA -3'	5'- CGGTAGACAGCGGCTATGTT -3'
Myo1e	5'- GGTTATGCTTATCGGCGTGT -3'	5'- CTTCTCCCAAGCTGGAACTG -3'
Tnip1	5'- AAGAGGAGGAGAAGGCCAAG -3'	5'- CCTTGTAGGCATGGTGAGGT -3'
Dhrsx	5'- GACCCTGTGACCTCCAACAT -3'	5'- CCTCCGACACCTTCTAGCTC -3'
Ddit4	5'- CTCTGGGATCGTTTCTCGTC -3'	5'- GACACCCCATCCAGGTATGA -3'
Cbr3	5'- ACACCCTTCGACATTCAAGC -3'	5'- TGCAGTTCTCAAGGGCTTTT -3'
Usp2	5'- CTTCTGGGATCTCTCGTTGC -3'	5'- TGTTGTGAGCTTGCTGGTTC -3'
Sgk1	5'- CATGCAAACACGCTGAAGTT -3'	5'- CCCTTTCCGATCACTTTCAA -3'
Ypel3	5'- AACCACGACGACCTCATCTC -3'	5'- GCTCATATTTCCAGCCCAAA -3'
Zfyve21	5'- GGGGACAGTCATCGTGAAAT -3'	5'- AGCTTGGTAGCCTTGTGCAT -3'
Ttf2	5'- GCCCAAAACTGAGAAAGCTG -3'	5'- ACCAAAAGCTGGGTTTCCTT -3'
Cutc	5'- TCGGATTGAACTGTGCTCTG -3'	5'- AAACCATCGGCACCATAAAG -3'
Tpd52	5'- ATTTTCATCGGTTGGCTCAG -3'	5'- TGTTCTGGAGGAGGCTCTGT -3'
GAPDH	5'- TGCACCACCAACTGCTTAG -3'	5'- GGATGCAGGGATGATGTTC -3'

entific), and signal intensities were quantified with a luminescent image analyzer (LAS-3000, Fuji Film, Tokyo, Japan). To determine intensities, immunoblotting images were scanned with Adobe Photoshop CS2 (Adobe Systems, San Jose, CA, USA) and quantified using ImageJ.

2.1.5 Validation of Gene Involvement by RNA Interference

To ensure the potential involvement of genes in osteoclastogenesis, silencing by RNA interference was performed. Cells were treated with siRNA specific to eIF2α Dusp2, Dscr1, Ptpn22, Sgk1, Ddit4, and Zfyve21 (Life Technologies). As a nonspecific control, a negative siRNA (Silencer Select #1, Life Technologies) was used. Cells were transiently transfected with siRNA for the specific genes or control in Opti-MEM I medium with Lipofectamine RNAiMAX (Life Technologies). Six hours later, the medium was replaced by regular culture medium. The efficiency of silencing was assessed with immunoblotting or quantitative PCR 48 hours after transfection.

2.1.6 miRNA Array Profiling

To obtain a list of microRNA potentially regulating osteoclastogenesis, a miRNA microarray was generated. The total RNA from RAW 264.7 samples treated with RANKL, RANKL+Salubrinal, and RANKl+Guanabenz were extracted after 4 hours of treatment. For miRNA array profiling, five g of total RNA from three control samples, three RANKL samples, three RANKL+Salubrinal samples, and three RANKL+Guanabenz samples were sent to LC Sciences (Houston, TX, USA) for miRNA array analysis using Sanger miRBase Release 16.0. Samples were analyzed using µParaflo Microfluidic Biochip Technology. Multiple redundant regions were included on the chip and each region further comprised a miRNA probe region plus multiple control probes. Statistics were done with ANOVA analysis.

2.1.7 mRNA Array Profiling

To obtain a list of genes potentially regulating osteoclastogenesis, an mRNA microarray was generated. For this, 250 g of total RNA from three control samples, three RANKL samples, three RANKL+Salubrinal samples, and three RANKL+Guanabenz samples were sent to OCI Genomics Center (Toronto, ON, CA). The samples were analyzed on Illumina MouseWG-6 v2.0 chip. The samples were labeled using Illu-

mina TotalPrep-96 RNA Amplification kit (Ambion). Hybridization onto two Mouse WG-6 V2 Beadchips was conducted using 1.5 ng of cRNA from each of the samples. The data was then imported in GeneSpring V12.5 for analysis. Statistics were done with one-way ANOVA.

2.1.8 Statistical Analysis

Three or four independent samples were conducted in each experiment and data were expressed as mean ± S.D. For comparison among multiple samples, ANOVA and post-hoc tests were conducted. Statistical significance was evaluated at $p < 0.05$. The single and double asterisks and daggers indicate $p < 0.05$ and $p < 0.01$, respectively.

2.2 *In Silico* Analysis

2.2.1 Gene Prediction Analysis

In order to predict potential stimulators and inhibitors of NFATc1 in response to the administration of salubrinal and guanabenz, we defined two parameters using genome-wide microarray data: distance, d_i, and root-mean-square (rms) p-value, p_i for gene i. The parameter d_i served as an indicator of resemblance ($d_i \approx 0$) and dissemblance ($d_i \approx 1$; reciprocal) to the mRNA expression profile of NFATc1, while the parameter p_i indicated representative statistical significance. The expression profiles of NFATc1 and gene i were evaluated under 4 culture conditions ($j = 1$ to 4), including control ($j = 1$), treatment with RANKL ($j = 2$), treatment of RANKL and salubrinal ($j = 3$), and treatment with RANKL and guanabenz ($j = 4$).

The distance, $(0 \leq d_i \leq 1)$, between NFATc1 and gene i, was defined using Pearson's correlation coefficient, r_i $(-1 \leq r \leq 1)$:

$$d_i = \frac{1 - r_i}{2} \tag{2.1}$$

$$r_i = \frac{\sum_{j=1}^{n} x_j y_{ij} - n\bar{x}\bar{y}_i}{\sqrt{\left(\sum_{j=1}^{n} x_j^2 - n(\bar{x})^2\right)\left(\sum_{j=1}^{n} y_j^2 - n(\bar{y}_i)^2\right)}} \tag{2.2}$$

where x_j represented NFATc1 mRNA levels for $j = 1$ to n $(n = 4)$, and y_{ij} was the mRNA levels of gene i for $j = 1$ to n. The variables $\bar{x}$ and $(\bar{y}_i)$ were the mean mRNA levels of x_j and y_{ij} for all values of j. The rms p-value, p_i, for gene i was defined:

$$p_i = \sqrt{\frac{(p_{iR})^2 + (p_{iS})^2 + (p_{iG})^2}{3}} \tag{2.3}$$

where p_{iR} was the p-value (Student's t-test) between $j = 1$ & 2, p_{iS} was the p-value between $j = 2$ & 3, and p_{iG} was the p-value between $j = 2$ & 4. To better visualize the prediction result, two plots of rms p-value (p_i) vs. distance (d_i) were generated using Excel, one of predicted stimulators and one of predicted inhibitors.

After making sure no repetition of genes occurs, a list of candidate genes was selected based on some criteria using fold change, f_{ij}, such that for gene i:

$$|f_{ij}| > 1.1 \text{ for } j = 2 \text{ to } 4 \tag{2.4}$$

$$f_{i2} < 0, f_{i3} \;\&\; f_{i4} > 0 \text{ or } f_{i2} > 0, f_{i3} \& f_{i4} < 0 \tag{2.5}$$

$$|f_{ij}| \leq |f_{i2}| \text{ for } j = 3 \text{ and } 4 \tag{2.6}$$

Note that f_{i1} for the control sample was defined to be 1, f_{i2} was determined with respect to $j = 1$ (control), and f_{i3} and f_{i4} to $j = 2$ (RANKL treatment). One-thousand-twenty-five genes were inputted into the analysis.

2.2.2 MicroRNA (miRNA) Prediction Analysis

A similar approach was established to predict potential miRNA stimulators and inhibitors of NFATc1 using the parameters d_m for distance and p_m for rms p-value

for miRNA m. The parameter d_m indicated the resemblance ($d_m \approx 0$) and dissemblance ($d_m \approx 1$) of the miRNA expressions to the NFATc1 expression profile, and the parameter p_m indicated statistical significance. The miRNA expressions were also evaluated under 4 culture conditions ($j = 1$ to 4): control ($j = 1$), treatment with RANKL ($j = 2$), treatment of RANKL and salubrinal ($j = 3$), and treatment with RANKL and guanabenz ($j = 4$). All miRNAs were analyzed except for the ones with p-value > 0.05 and signals < 500.

The distance, d_m ($0 \leq d_m \leq 1$), between NFATc1 and miRNA m, was also defined using Pearson's correlation coefficient, r_m ($-1 \leq r_m \leq 1$):

$$d_m = \frac{1 - r_m}{2} \tag{2.7}$$

$$r_m = \frac{\sum_{j=1}^{n} x_j y_{mj} - n\bar{x}\bar{y}_m}{\sqrt{\left(\sum_{j=1}^{n} x_j^2 - n(\bar{x})^2\right)\left(\sum_{j=1}^{n} y_j^2 - n(\bar{y}_m)^2\right)}} \tag{2.8}$$

where x_j represented NFATc1 expression levels for $j = 1$ to n ($n = 4$), and y_{mj} was the expression levels of miRNA m for $j = 1$ to n. The variables $\bar{x}$ and $\bar{y}_m$ were the mean expression levels of x_j and y_{mj} for all values of j. The rms p-value, p_m, for miRNA m was defined:

$$p_m = \sqrt{\frac{(p_{mR})^2 + (p_{mS})^2 + (p_{mG})^2}{3}} \tag{2.9}$$

where p_{mR} = p-value (Student's t-test) between $j = 1$ & 2, p_{mS} = p-value between $j = 2$ & 3, and p_{mG} = p-value between $j = 2$ & 4. To better visualize the prediction result, two plots of rms p-value (p_m) vs. distance (d_m) were generated using Excel, one of predicted stimulator miRNAs and one of predicted inhibitor miRNAs. One-thousand-two-hundred-sixty-five microRNAs were inputted into the analysis.

Further analysis was conducted to see if the predicted miRNAs could potentially target the predicted mRNAs using miRNA_Targets, a target prediction computational tool. All of the predicted miRNAs were analyzed at each available binding energy using both the miRanda and RNA hybrid algorithms. Using a Perl script, the output genes of the target prediction analysis were examined for matches with our predicted

stimulators and inhibitors including the lowest binding energy at which it was found. The results were put into a table for ease of observation.

3. RESULTS

3.1 Inhibition of Osteoclastogenesis in RAW264.7 Cells by Salubrinal and Guanabenz

In response to 0.1–20 µM salubrinal for 24 h, we examined cell mortality and live cell numbers of RAW264.7 pre-osteoclasts. Cell mortality ratio did not present statistically significant differences in the presence and absence of RANKL (Fig. 3.1). The number of live cells was increased by ∼50% by incubation with RANKL, and

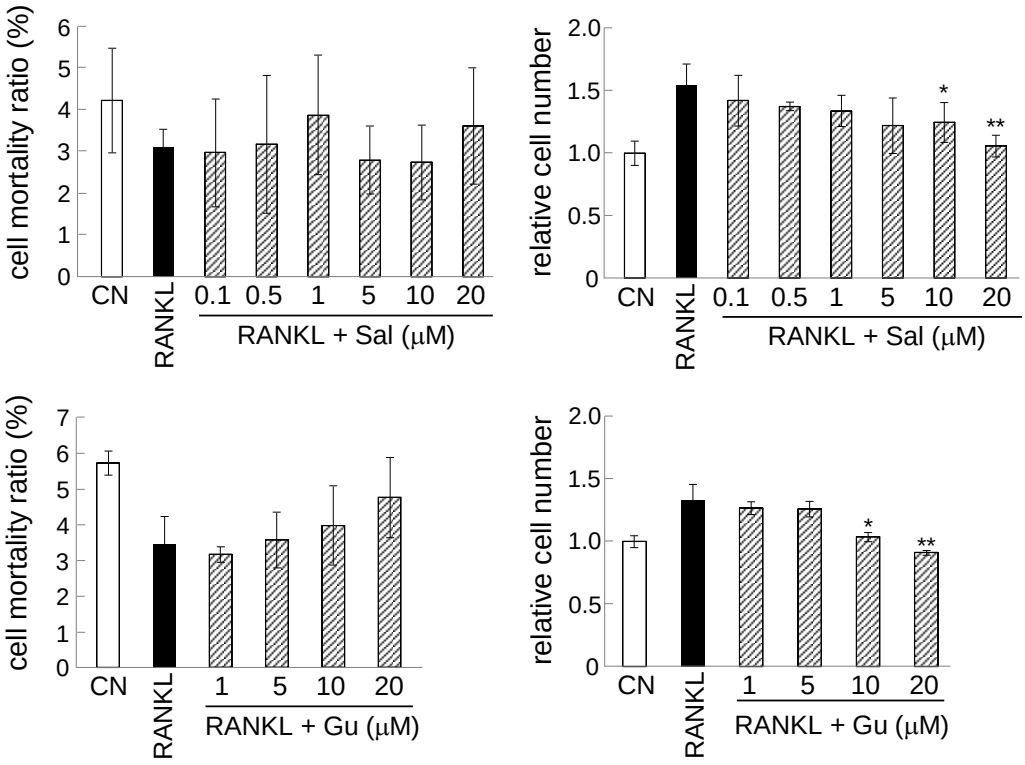

Fig. 3.1. Effect on cell mortality and relative cell number after the addition of salubrinal (Sal,top) and guanabenz (Gu,bottom).

administration of 10–20 µM salubrinal reduced the numbers approximately by 10%. Similar to salubrinal, administration of 1 and 5 µM guanabenz did not alter cell mortality and the number of live cells, although its administration at 10 and 20 µM reduced the number of live cells in 24 h. With the stimulatory role of RANKL, the number of TRAP-positive multi-nucleated cells was significantly increased by the addition of RANKL. However, administration of 0.5 µM to 20 µM salubrinal reduced the number of TRAP-positive cells in a dose-dependent manner (Fig. 3.2A). Consistent with salubrinal's inhibitory action, guanabenz also attenuated osteoclastogenesis of RAW264.7 cells in a dose-dependent manner. Compared to the number of TRAP-positive multi-nucleated cells of 377 ± 39 (RANKL only), guanabenz reduced the number of differentiated osteoclasts to 364 ± 38 (1 µM), 288 ± 51 (5 µM), 189 ± 25 (10 µM), and 73 ± 16 (20 µM) (Fig. 3.2B).

3.2 Downregulation of NFATc1 in RAW 264.7 Cells by Salubrinal and Guanabenz

Addition of RANKL to the culture medium significantly induced NFATc1 production (Fig. 2A). The RANKL-induced protein expression of NFATc1 was reduced by the administration of 5–20 µM salubrinal at day 2 and maintained its elevated level on day 4 (Fig. 3.3A). Administration of 10–20 µM guanabenz after 2 days showed a similar result, and the effect of both salubrinal and guanabenz was dose-dependent (Fig. 3.3B).

3.3 Reduction of RANKL-induced NFATc1, C-fos, TRAP, and OSCAR

Addition of RANKL also increased the mRNA levels of NFATc1, TRAP, and OSCAR, and administration of 20 µM salubrinal significantly reduced their mRNA levels (Fig. 3.4). On day 2 for instance, the RANKL-driven increase was 9.4 ± 0.5 fold (NFATc1), 1.9 ± 0.1 fold (c-fos), 165 ± 4.2 fold (TRAP), and 467 ± 22 fold (OSCAR). The reduction by 20 µM salubrinal was 46% (NFATc1), 32% (c-fos), 35% (TRAP), and 21% (OSCAR). Consistent with the observed dose response, administration of

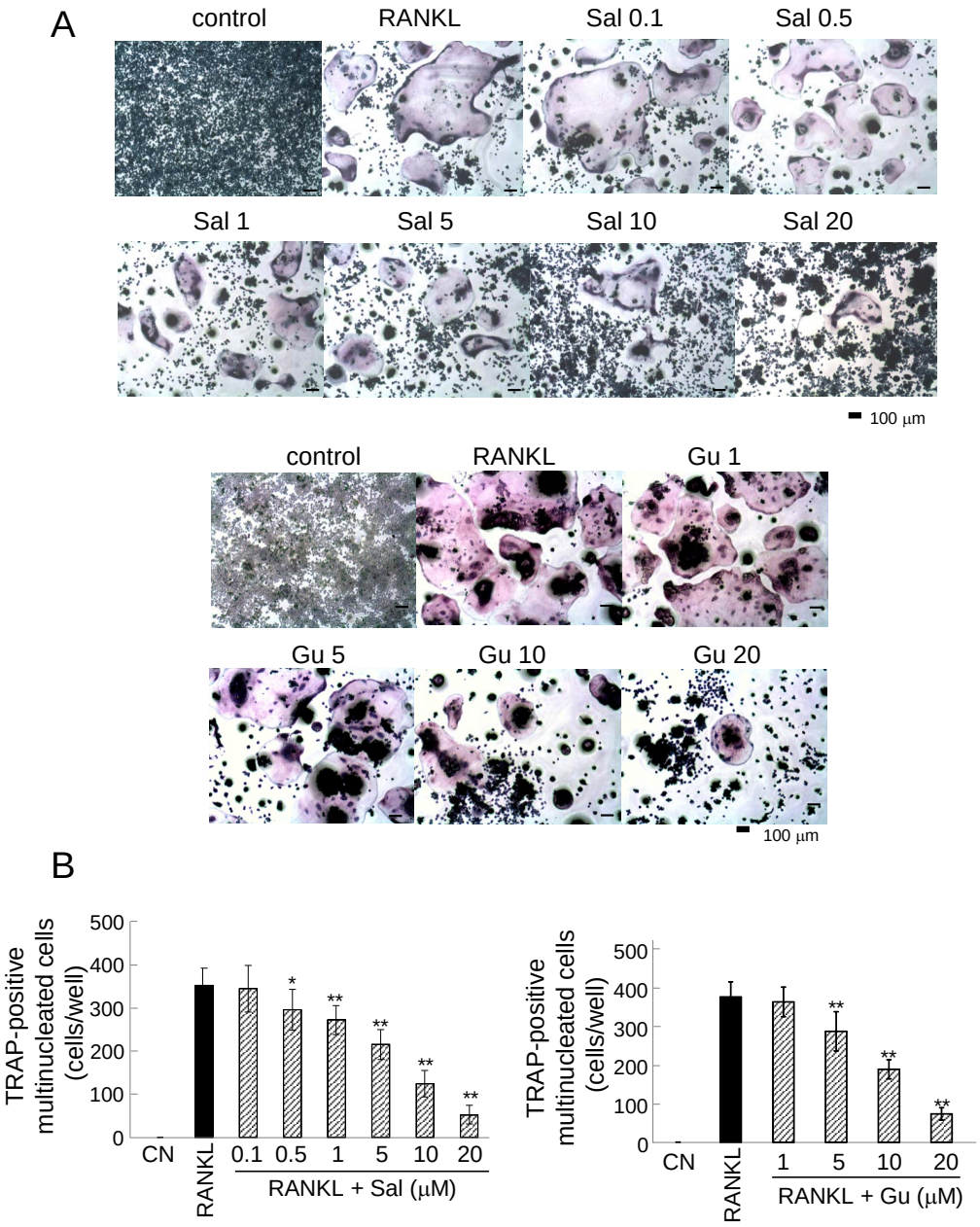

Fig. 3.2. Inhibitory effects of salubrinal on RANKL-driven maturation of RAW264.7 pre-osteoclasts. CN = control, and Sal = salubrinal. The single and double asterisks indicate $p < 0.05$ and $p < 0.01$ in comparison to the RANKL-treated cells, respectively. (A) Dose-dependent suppression of RANKL driven activation of osteoclasts by salubrinal and guanabenz. (B) Dose-dependent suppression of TRAP-positive multi-nucleated cells by salubrinal and guanabenz.

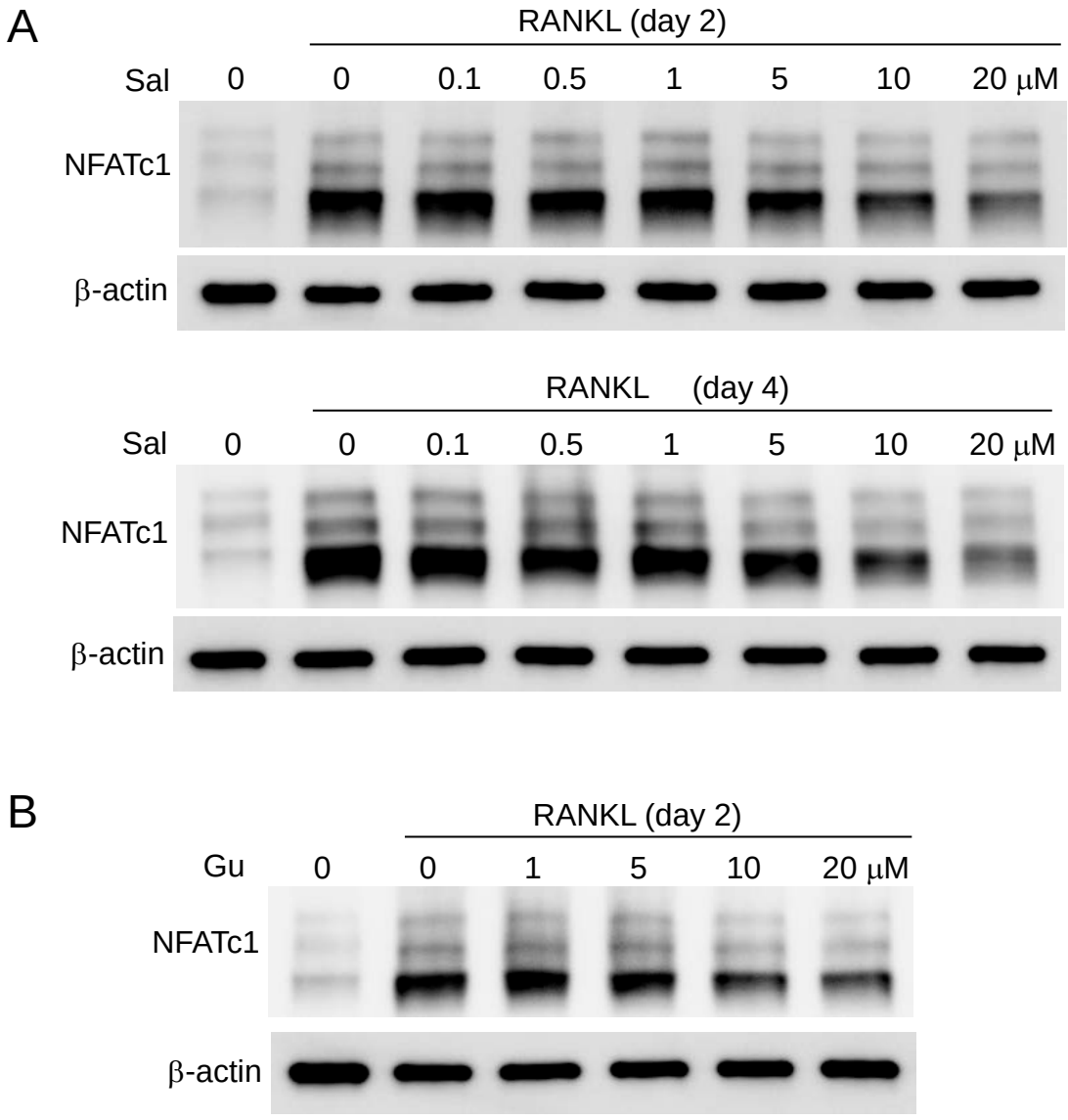

Fig. 3.3. Reduction of RANKL-induced NFATc1 on protein expression by salubrinal and guanabenz. (A) Expression of NFATc1 2 days and 4 days after RANKL and salubrinal (B) Expression of NFATc1 2 days after RANKL and guanabenz.

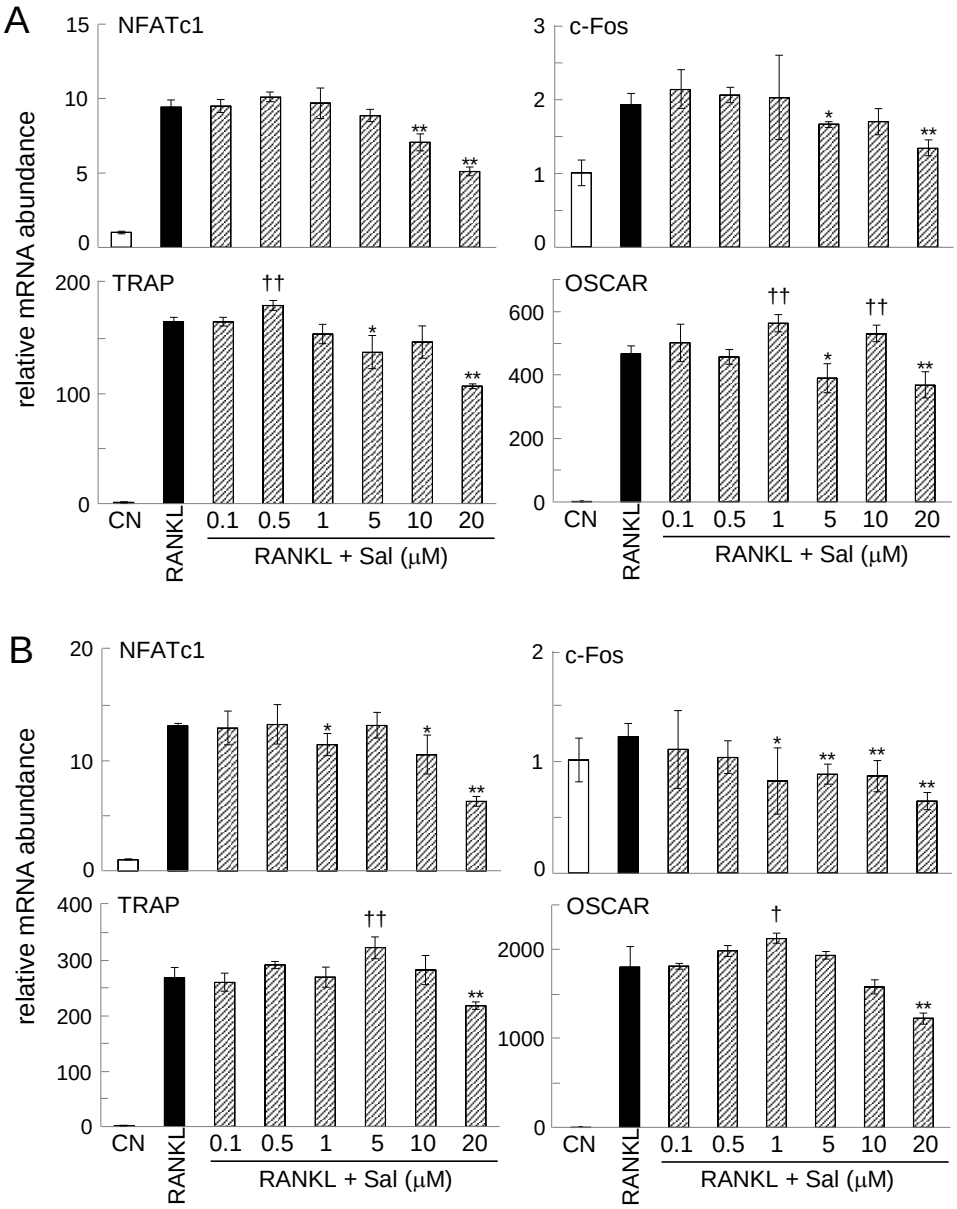

Fig. 3.4. Effects of salubrinal on mRNA expression levels of NFATc1, c-Fos, TRAP, and OSCAR. CN = control. The single and double asterisks indicate significant decreases with $p < 0.05$ and $p < 0.01$ in comparison to the RANKL-treated cells, respectively. The single and double daggers indicate significant increases with $p < 0.05$ and $p < 0.01$ in comparison to the RANKL-treated cells, respectively. (A) Messenger RNA levels (2 days after RANKL administration). (B) Messenger RNA levels (4 days after RANKL administration).

salubrinal at 0.1–1 μM did not contribute to significant reduction in these mRNA levels except for NFATc1 and c-fos on day 4. The RANKL-induced mRNA levels of NFATc1, c-Fos, TRAP, and OSCAR were also reduced by administration of 20 μM guanabenz (Fig. 3.5).

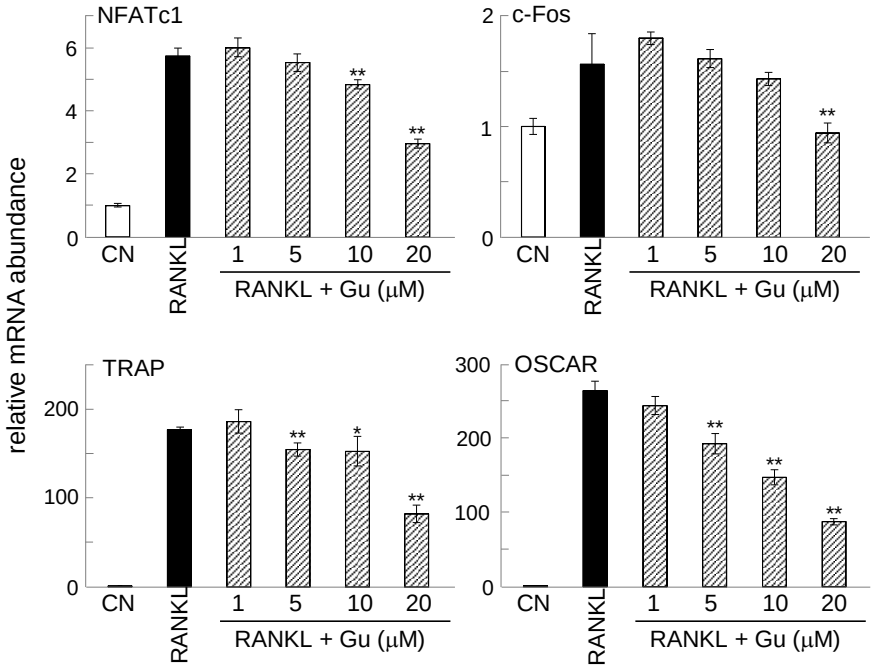

Fig. 3.5. Effects of guanabenz on mRNA expression levels of NFATc1, c-Fos, TRAP, and OSCAR. CN = control. The single and double asterisks indicate significant decreases with $p < 0.05$ and $p < 0.01$ in comparison to the RANKL-treated cells, respectively.

3.4 Temporal Profile of P-eIF2α and NFATc1

The temporal expression profile revealed that the addition of RANKL transiently reduced the phosphorylation level of eIF2α (2–8 h) and elevated NFATc1 by 13.4 ± 3.2 fold (24 h) (Fig. 3.6A). This induction of NFATc1 was partially suppressed by salubrinal with an increase in the level of p-eIF2α. In the early period (2–4 h), administration of 20 μM salubrinal increased the level of p-eIF2α but did not alter the level of NFATc1. In the later period (8–24 h), however, the level of NFATc1 was

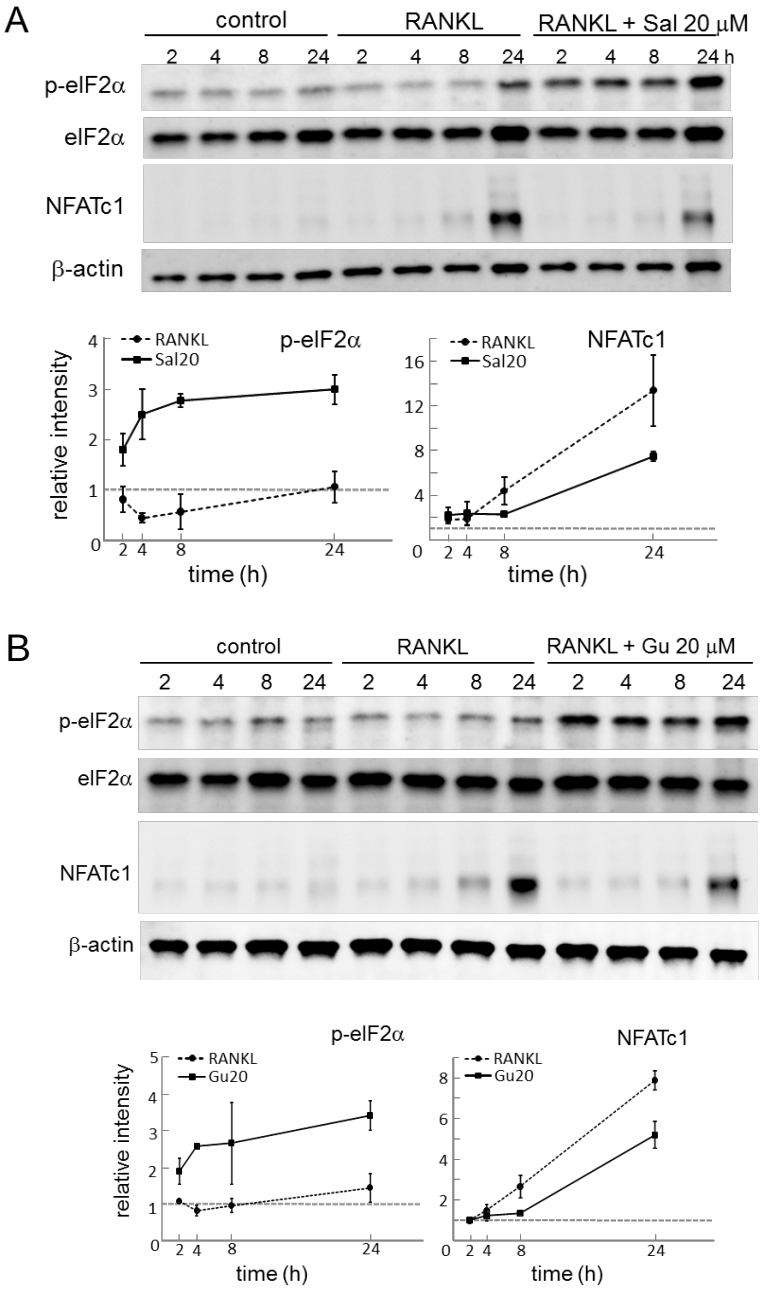

Fig. 3.6. Evaluation of the potential involvement of eIF2α in salubrinal and guanabenz-driven down-regulation of NFATc1. (A) Western blot analysis of p-eIF2α and NFATc1 with and without 20 μM (A) salubrinal and (B) guanabenz. The normalized level of 1 was defined as the level for the cells that were not treated with RANKL without administration of salubrinal or guanabenz.

significantly reduced by 48% (8 h) and 44% (24 h) (Fig. 3.6A). Similar to the effect from salubrinal, the temporal expression profile of p-eIF2α and NFATc1 in response to 20 µM guanabenz revealed that p-eIF2α was upregulated in 2 h, and NFATc1 was partially suppressed in 8 h (Fig. 3.6B).

3.5 Recovery of NFATc1 Expression by RNA Interference for eIF2α

To evaluate the effects of eIF2α on the expression of NFATc1, we employed RNA interference specific for eIF2α and compared it to a non-specific control (NC) (Fig. 3.7A). In response to 20 µM salubrinal, RAW264.7 cells transfected with the control siRNA demonstrated a reduction of NFATc1 by 56%. However, the expression of NFATc1 was reduced only by 20% in the cells transfected with eIF2α siRNA. Furthermore, 20 µM guanabenz decreased the level of NFATc1 by 43% in the cells transfected with the control siRNA but the transfection of eIF2α siRNA abolished the suppressive effect of guanabenz (Fig. 3.7B & 3.7C). The phosphorylation level of NFχB was not significantly altered by transfection with eIF2α siRNA.

3.6 Effect of Salubrinal and Guanabenz on Some Known Signaling Pathways

Administration of 20 µM salubrinal did not significantly alter the RANKL-induced phosphorylation level of ERK, p38 MAPK, and NFχB (Fig. 3.8). However, administration of salubrinal increased the phosphorylation level of eIF2α in 15 min.

3.7 NFATc1 Expression Pattern and the Predicted Regulatory Network

To further identify the genes potentially targeted by salubrinal and guanabenz to regulate NFATc1, we employed in silico mRNA analysis. Since NFATc1 is the main focus of this study, its expression pattern is used as a base line for the analysis. Figure 3.9A shows the NFATc1 expression pattern is significantly up-regulated by RANKL treatment, reduced by 15% after addition of salubrinal, and significantly reduced by

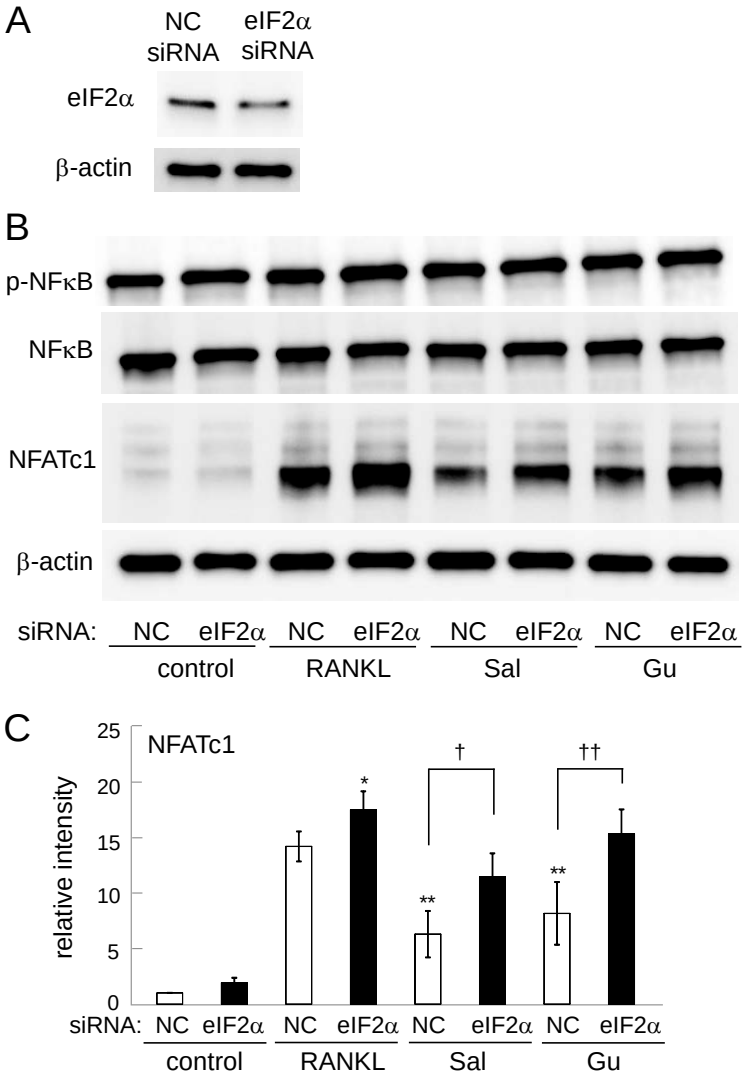

Fig. 3.7. Reduction in salubrinal/guanabenz-driven suppression of NFATc1 expression by RNA interference specific for eIF2α. Sal = salubrinal, Gu = guanabenz, and NC = non-specific control siRNA. The single and double asterisks indicate significant changes to the RANKL-treated NC siRNA cells with $p < 0.05$ and $p < 0.01$, respectively. The single and double daggers indicate significant changes to the salubrinal or guanabenz-treated NC siRNA cells with $p < 0.05$ and $p < 0.01$, respectively. (A) eIF2α level after transfecting siRNA specific to eIF2α. (B) Western blot analysis of p-NFκB and NFATc1. (C) Comparison of the expression level of NFATc1 between control siRNA and eIF2α siRNA.

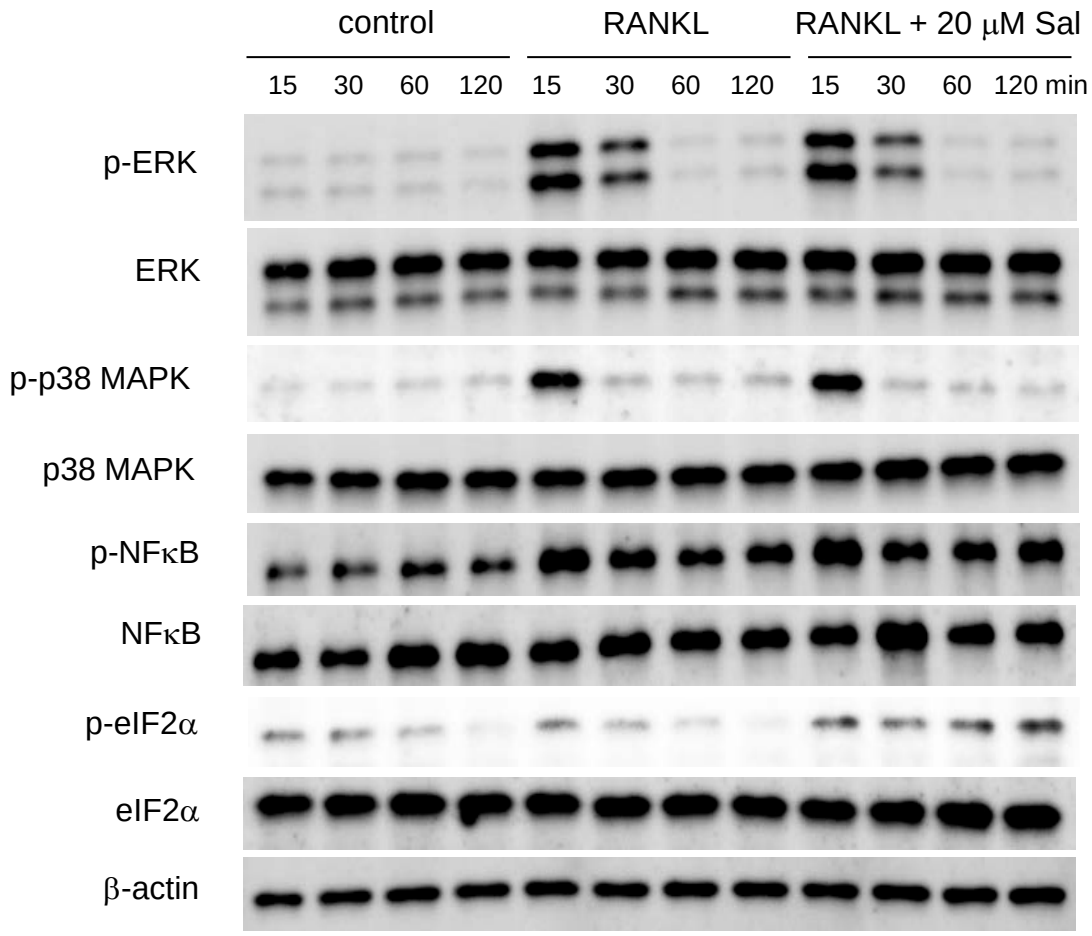

Fig. 3.8. Temporal expression profile of p-ERK, p-p38 MAPK, p-NFκB, p-eIF2α , and NFATc1 in the presence and absence of 20 μM Salubrinal. Western blot analysis of p-ERK, p-p38 MAPK, p-NFκB, and p-eIF2α at 15, 30, 60, and 120 min.

57% after addition of guanabenz. The similar expression pattern of NFATc1 mRNA after 4 hr treatment, which is the length of time chosen for microarray samples, is shown in the proposed regulatory network for salubrinal/guanabenz regulation of NFATc1 (Fig. 3.9B). A1 and B1 pathway: salubrinal / guanabenz directly regulates the inhibitor / stimulator genes of NFATc1. A2 and B2 pathway: salubrinal / guanabenz regulates inhibitor / stimulator genes of NFATc1 through activating / de-activating microRNAs.

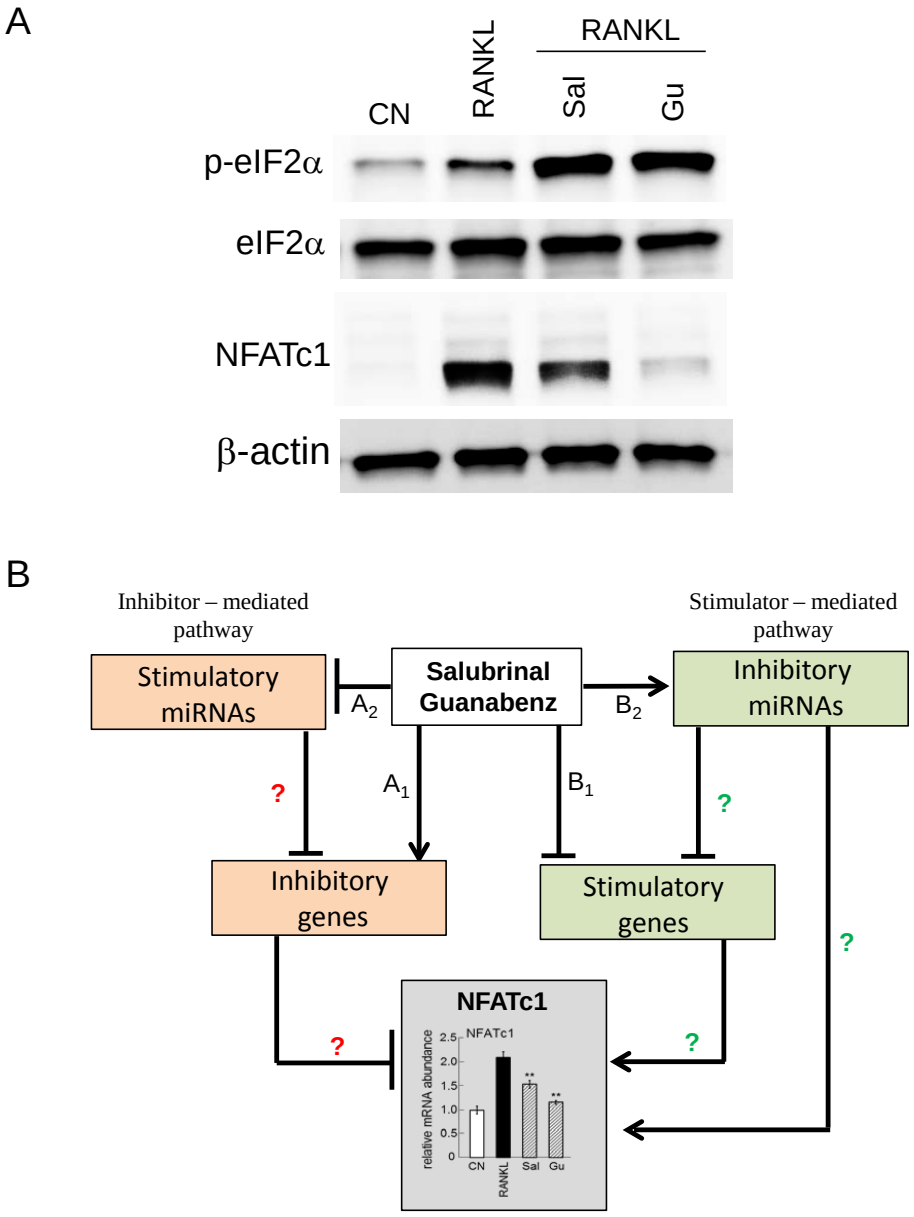

Fig. 3.9. Schematic of the predicted regulatory network. (A) Western blot analysis of NFATc1 after 24 hours treatment of RANKL, RANKL + salubrinal, and RANKL + guanabenz. This NFATc1 pattern is used to categorize the mRNA and miRNA expression patterns. (B) Predicted regulatory network for salubrinal/guanabenz-driven down-regulation of NFATc1.

3.8 Predicted mRNAs Regulating NFATc1

Figure 3.10 shows the plot of the output from the mRNAs MatLab prediction program for potential stimulators and inhibitors. Note that the closer the distance value of an mRNA to the minimum distance (0), the more similar its expression pattern is to NFATc1. On the other hand, the closer the distance value is to the maximum distance (1), the more opposite its expression pattern is to NFATc1. The stimulator group has the furthest distance of 0.097 from NFATc1, while the inhibitor group has the furthest distance of 0.903 from the reciprocal of NFATc1. Evaluation of a set of candidates with significant rms p-value (< 0.05) was conducted. From 1025 genes, 57 regulators were predicted which includes 40 stimulatory and 17 inhibitory genes.

3.9 qPCR Validation of Potential Stimulators and Inhibitors of NFATc1

Using qPCR, an expression pattern of 17 stimulatory and 9 inhibitory genes were confirmed. Dscr1, Dusp2, Ptpn22, Jdp2, Adora2b, and Syt16 was confirmed to have similarity to that of NFATc1 (Fig. 3.11 and 3.12). The other set of genes such as Zfyve2, Ypel3, Ddit4, Sgk1, Cbr3, and Usp2 were confirmed to have their opposite expression pattern to that of NFATc1 (Fig. 3.13 and 3.14).

The diagram in Figure 3.15 shows the predicted NFATc1 regulatory pathway with the qPCR validated genes as the potential NFATc1 regulators. These validated genes need to be further validated, including a loss-of-function assay by RNA interference. If none of these validated genes are confirmed to be an inhibitor of NFATc1, more candidates could be chosen, validated, and analyzed from the pool of potential regulating genes (gray circles, Fig. 3.12 and 3.14).

3.10 Validation of Zfyve21 and Ddit4 as Potential Inhibitors of NFATc1

Further confirmation using RNA interference did not validate some of the genes, however, Zfyve21 and Ddit4 showed potential involvement as NFATc1 inhibitors (Fig.

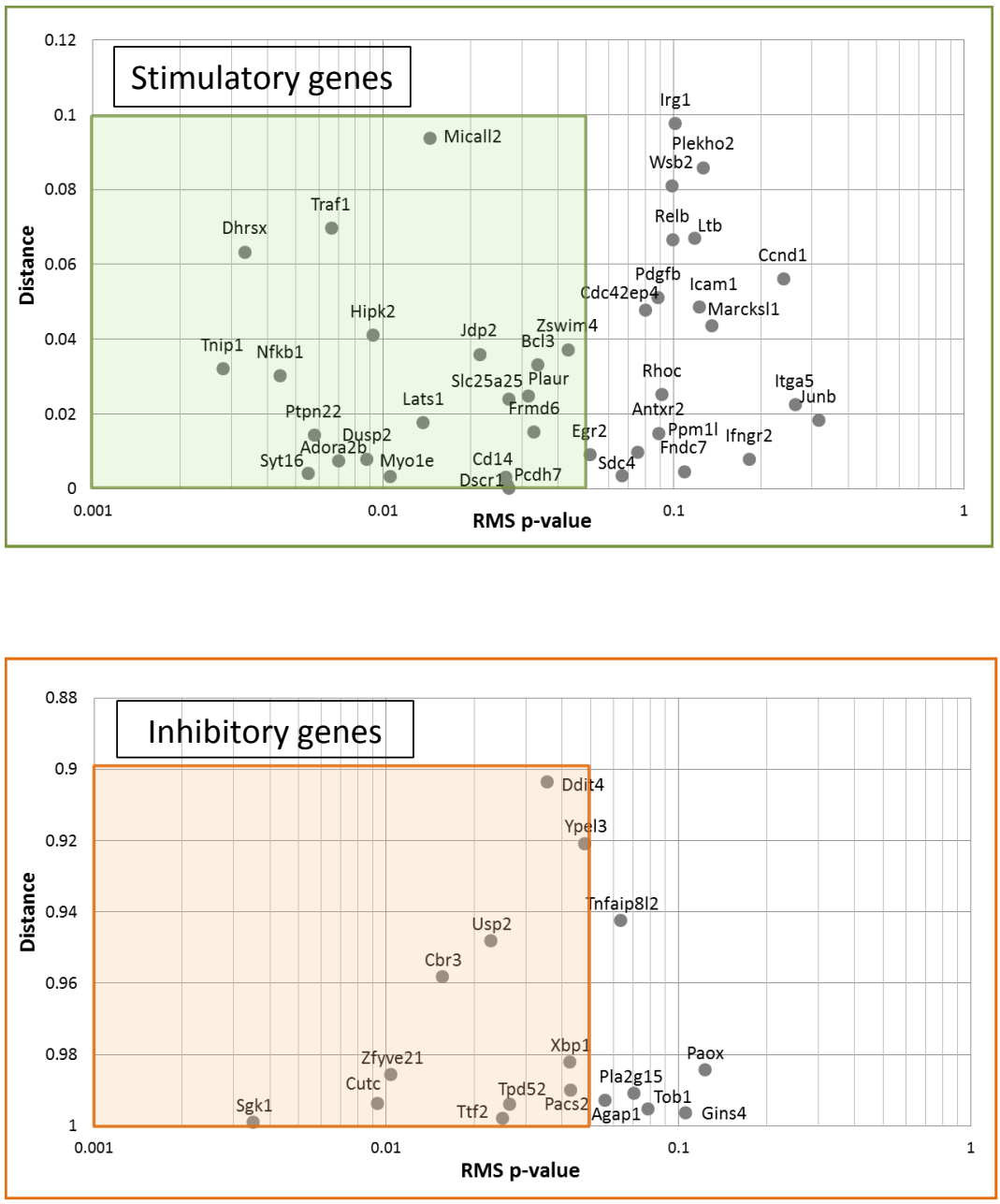

Fig. 3.10. Global identification of stimulatory and inhibitory genes in the distance vs. rms p-value plane. (Top) mRNAs having the same expression pattern as NFATc1 (stimulators). (Bottom) mRNAs having the opposite expression pattern as NFATc1 (inhibitors). Shaded areas indicate genes with $p < 0.05$.

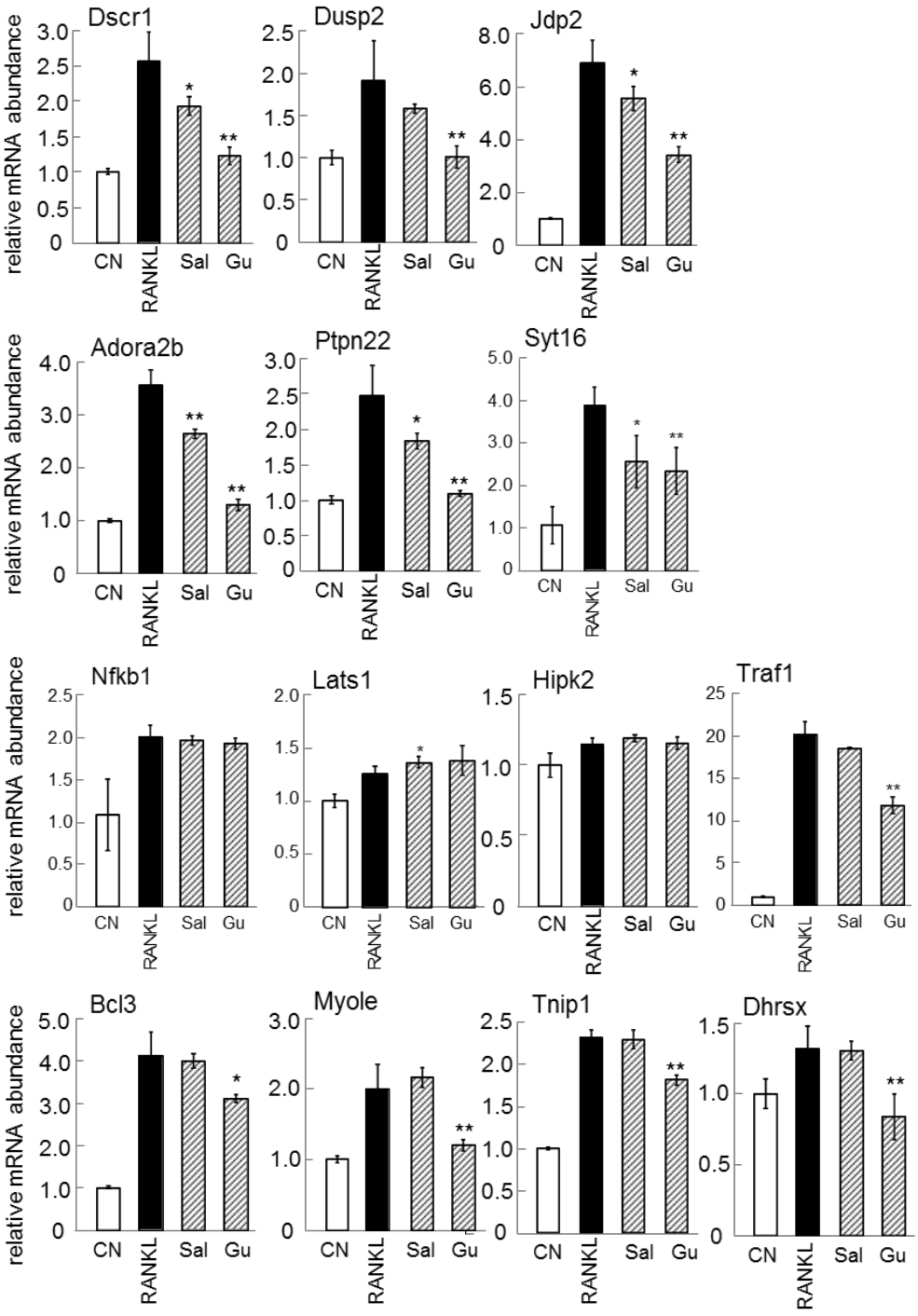

Fig. 3.11. mRNA levels of the predicted stimulators having significant p-value ($p < 0.05$).

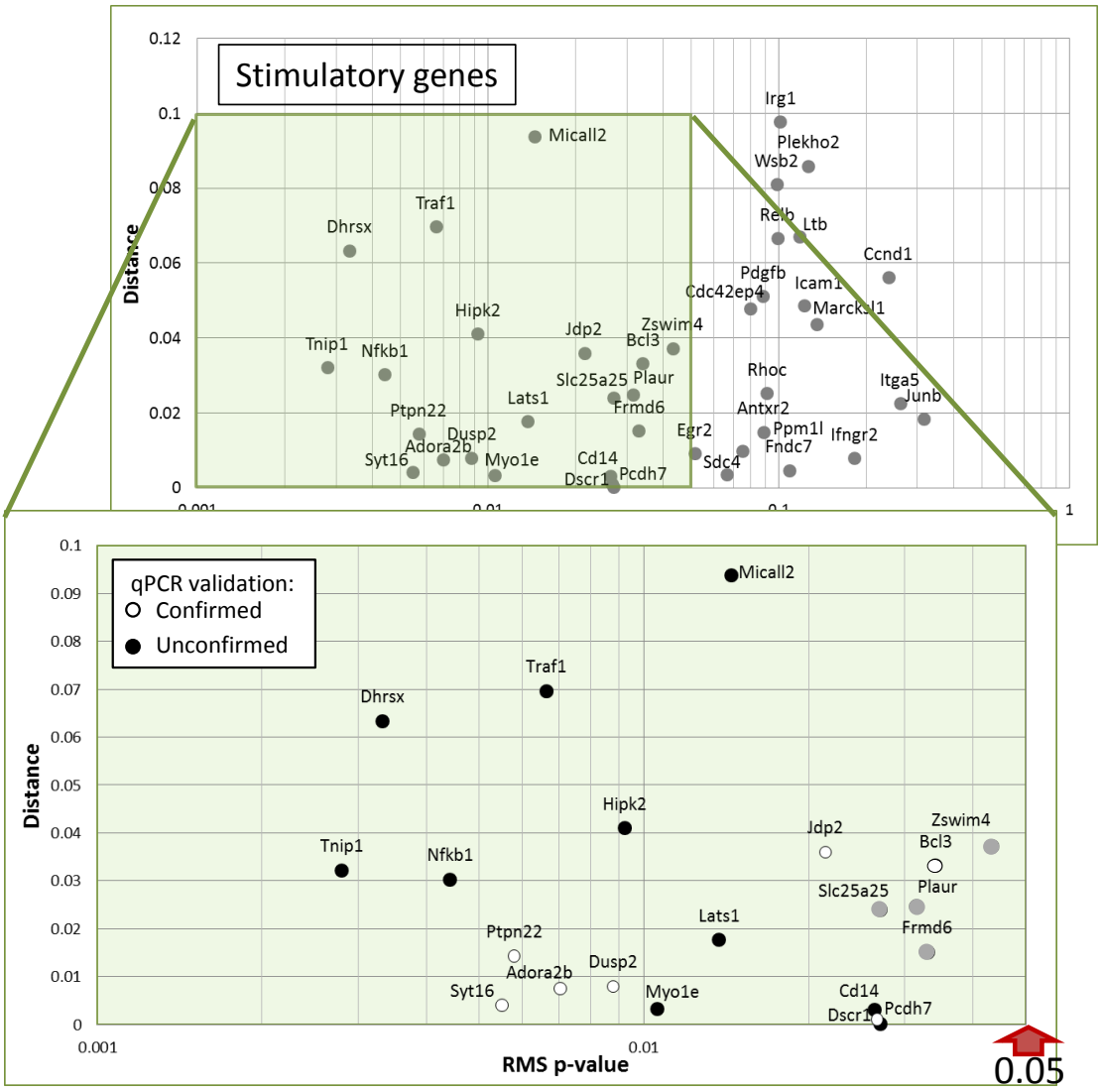

Fig. 3.12. Predicted stimulators validated by qPCR having $p < 0.05$. Hollow, black, and gray circles represent confirmed, unconfirmed, and not yet confirmed stimulators, respectively.

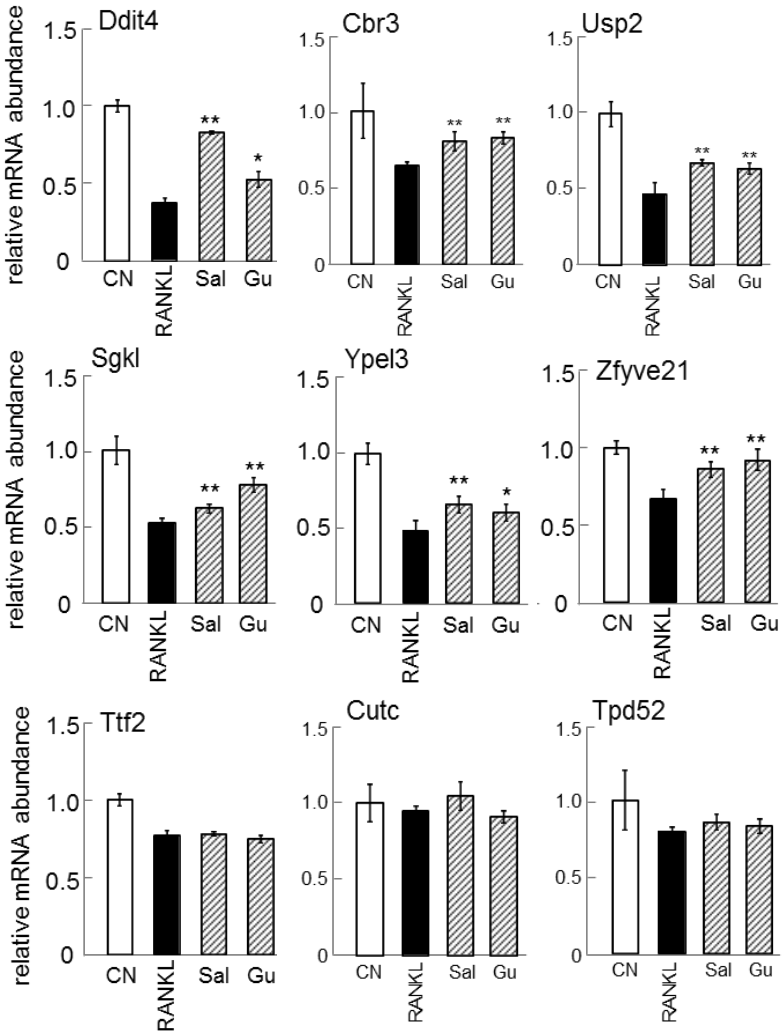

Fig. 3.13. mRNA levels of the predicted inhibitors having significant p-value ($p < 0.05$).

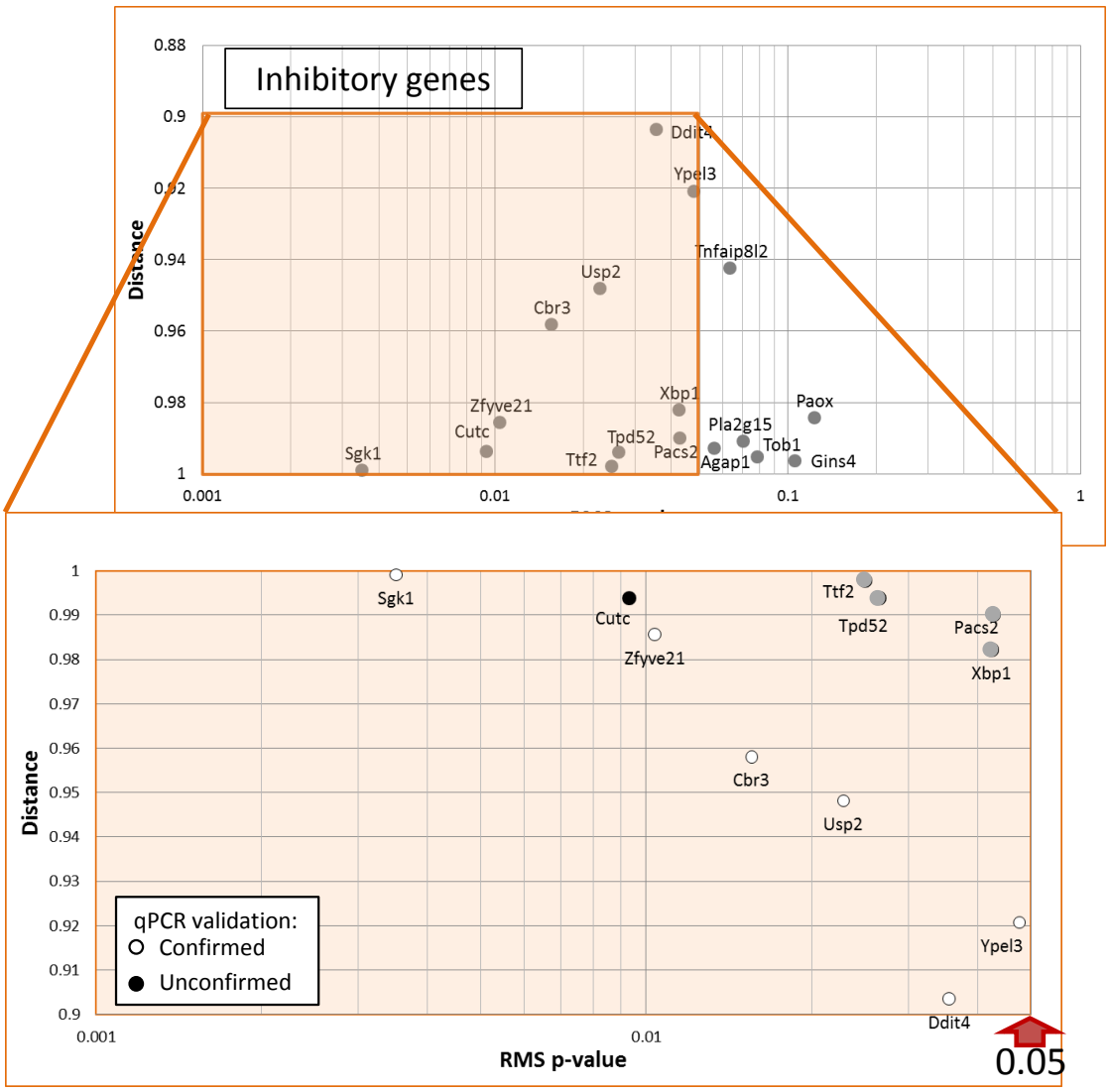

Fig. 3.14. Predicted inhibitors validated by qPCR having $p < 0.05$. Hollow, black, and gray circles represent confirmed, unconfirmed, and not yet confirmed stimulators, respectively.

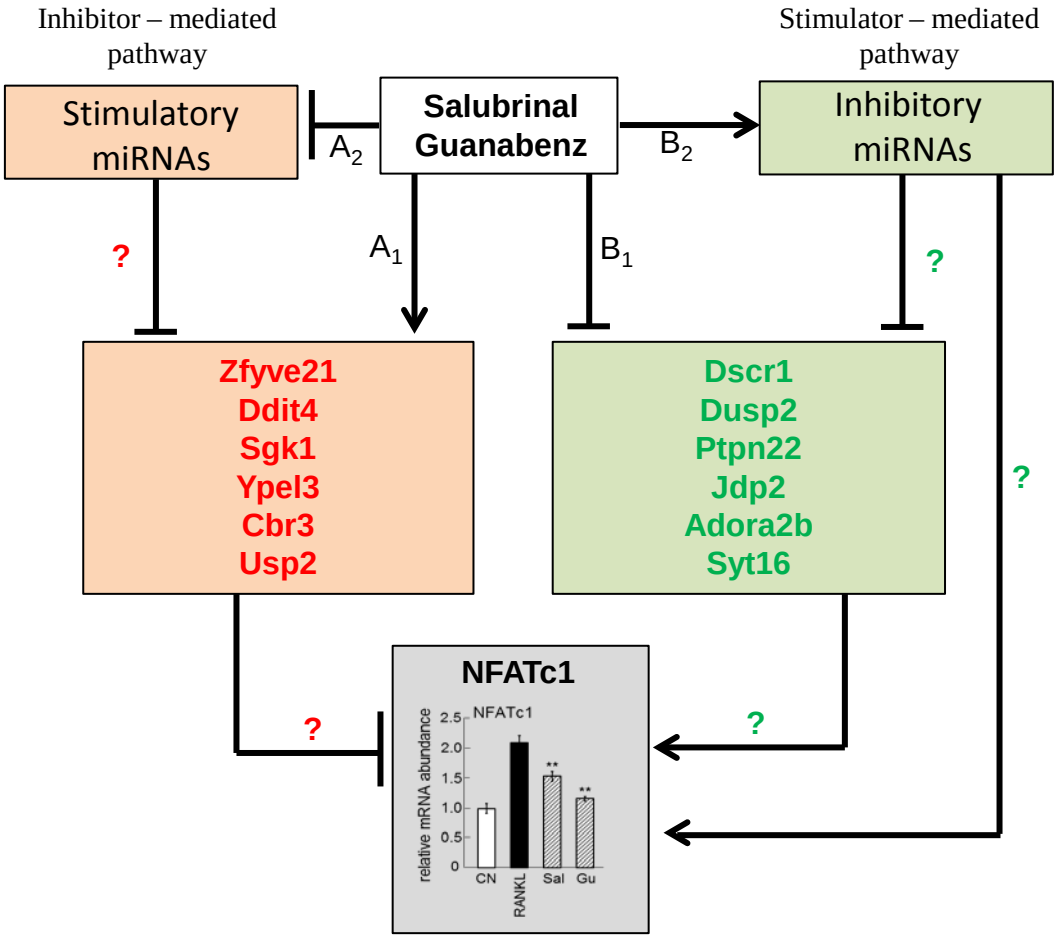

Fig. 3.15. Schematic of the predicted regulatory network with genes confirmed by qPCR validation

3.16 and 3.17). Figures 3.16B and 3.17B show the effectiveness of siRNA in suppressing the expression of Zfyve21 and Ddit4 after 72 hr of siRNA transfection. In Figure 3.16C, treatment of 20 µM guanabenz reduced the NFATc1 expression by 36% compared to RANKL treatment, but the transfection of Zfyve21 siRNA nearly abolished the suppressive effect of guanabenz. A similar result was observed with Ddit4 siRNA samples (Fig. 3.17C). Treatment of 20 µM salubrinal decreased the level of NFATc1 expression by 72% compared to RANKL treatment but recovered by 25% in Ddit4 siRNA samples. Western blot results also showed significant reduction in the suppressive effect of salubrinal and guanabenz in the samples treated with Zfyve21 and Ddit4 siRNA (Fig 3.16D and 3.17D). The genes such as Zfyve21 and Ddit4, which showed potential involvement after RNA interference, should be further validated using a gain-of-function assay by plasmid overexpression.

3.11 Predicted MicroRNAs Regulating NFATc1

Similar to the mRNAs, the miRNAs were correlated to NFATc1 and divided into stimulator and inhibitor groups (Fig. 3.18). Again, distance values of 0 indicated similarity with the NFATc1 expression pattern, and distance values of 1 indicate expression patterns opposite to NFATc1. The more likely candidates are said to be the ones with a distance value less than 0.3 or greater than 0.7. Many candidates with significant rms p-values are shown in the NFATc1-like group, but only one, miR-5109, is found with significant rms p-value in the NFATc1-reciprocal group. Regardless of the significance of the rms p-values, miRNAs with small distance values (< 0.3 or > 0.7) were analyzed with the target prediction tool.

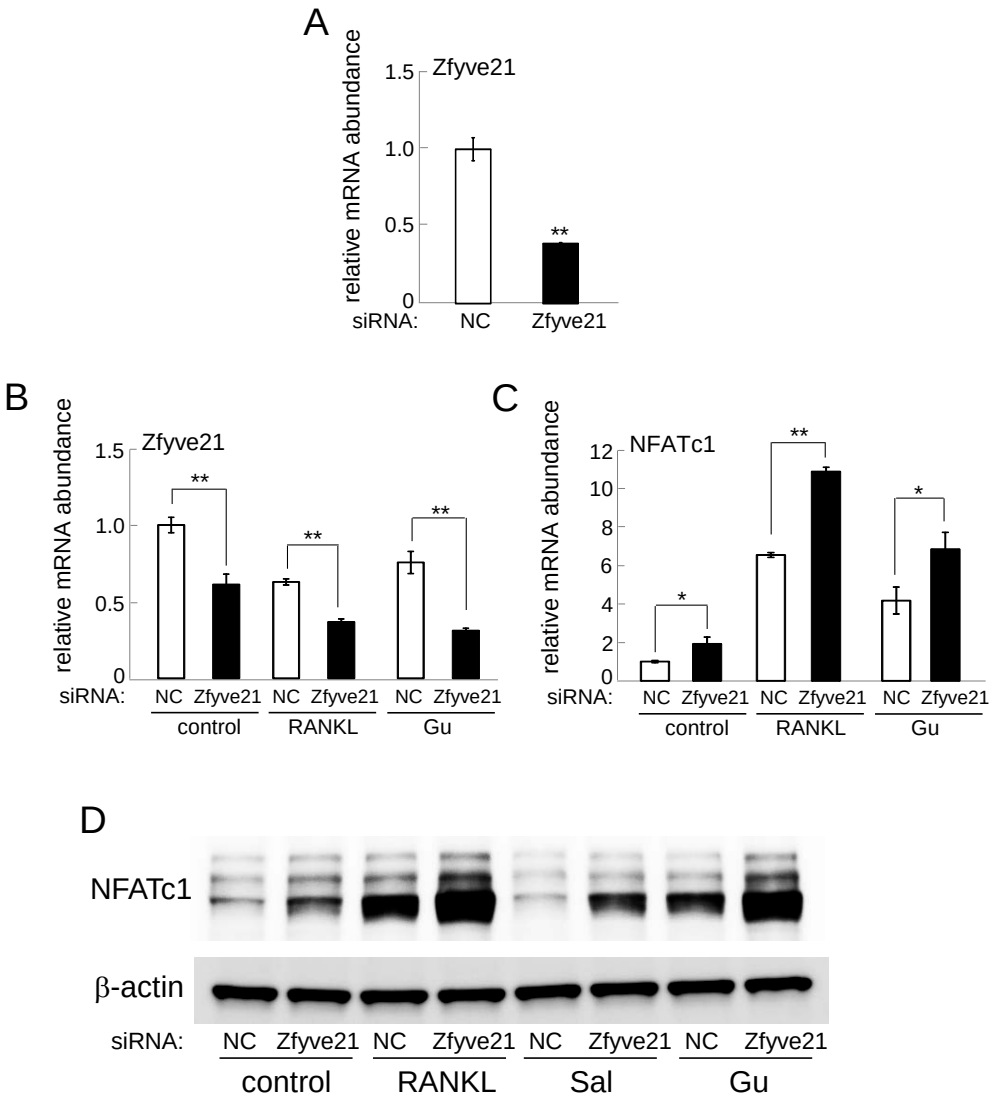

Fig. 3.16. Evaluation of Zfyve21 as a potential inhibitor of NFATc1 in response to salubrinal and guanabenz. The single and double asterisks indicate significant changes to the RANKL-treated NC siRNA cells with $p < 0.05$ and $p < 0.01$, respectively. (A) Zfyve21 level after transfecting with siRNA specific to Zfyve21 for 48 hr. (B) Expression level of Zfyve21 on control, RANKL, and RANKL + guanabenz treated samples between negative control siRNA and Zfyve21 siRNA after 72 hr. (C) Comparison of NFATc1 expression level between negative control siRNA and Zfyve21 siRNA on control, RANKL, and RANKL + guanabenz treated samples. (D) Western blot analysis of NFATc1 between negative control siRNA and Zfyve21 siRNA on control, RANKL, RANKL + salubrinal, and RANKL + guanabenz samples.

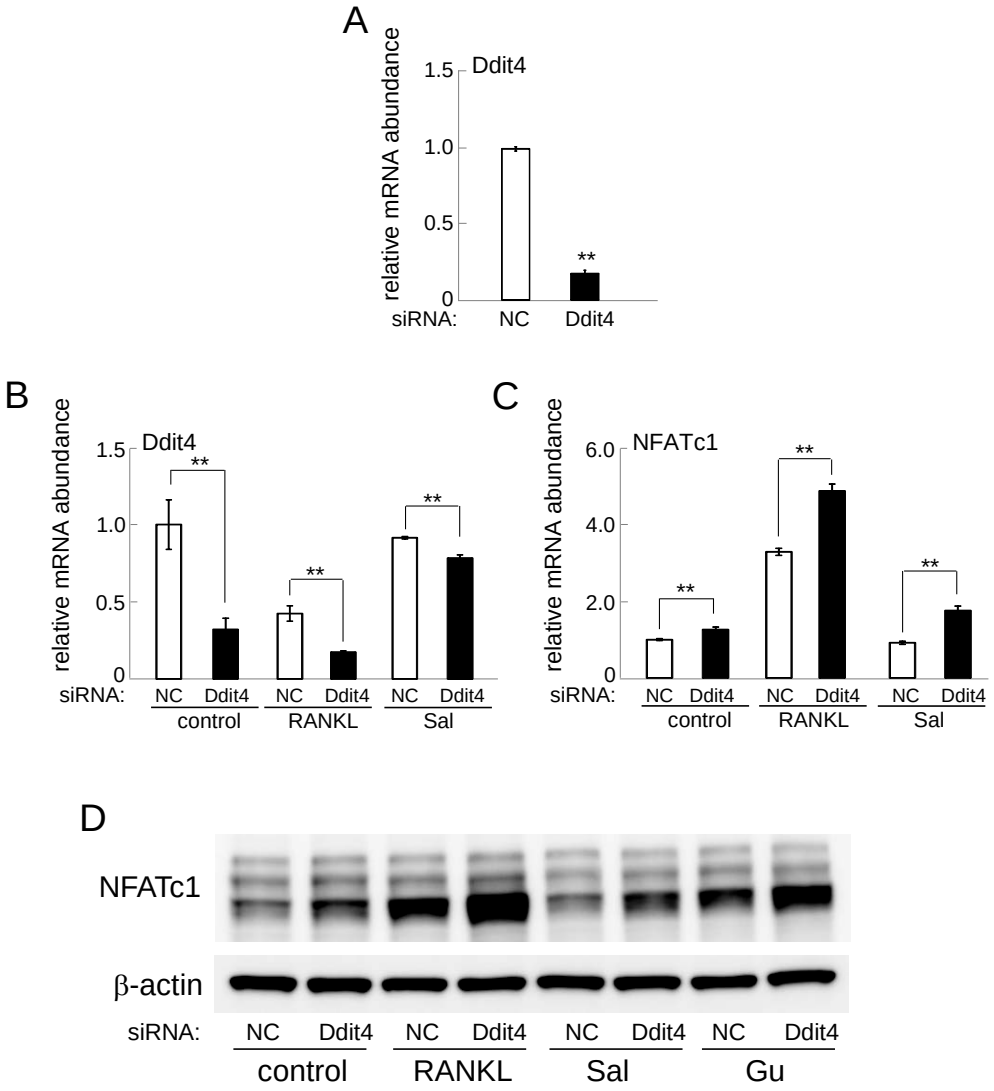

Fig. 3.17. Evaluation of Ddit4 as a potential inhibitor of NFATc1 in response to salubrinal and guanabenz. The single and double asterisks indicate significant changes to the RANKL-treated NC siRNA cells with $p < 0.05$ and $p < 0.01$, respectively. (A) Ddit4 level after transfecting with siRNA specific to Ddit4 for 48 hr. (B) Expression level of Ddit4 on control, RANKL, and RANKL + guanabenz treated samples between negative control siRNA and Ddit4 siRNA after 72 hr. (C) Comparison of NFATc1 expression level between negative control siRNA and Ddit4 siRNA on control, RANKL, and RANKL + guanabenz treated samples. (D) Western blot analysis of NFATc1 between negative control siRNA and Ddit4 siRNA on control, RANKL, RANKL + salubrinal, and RANKL + guanabenz samples.

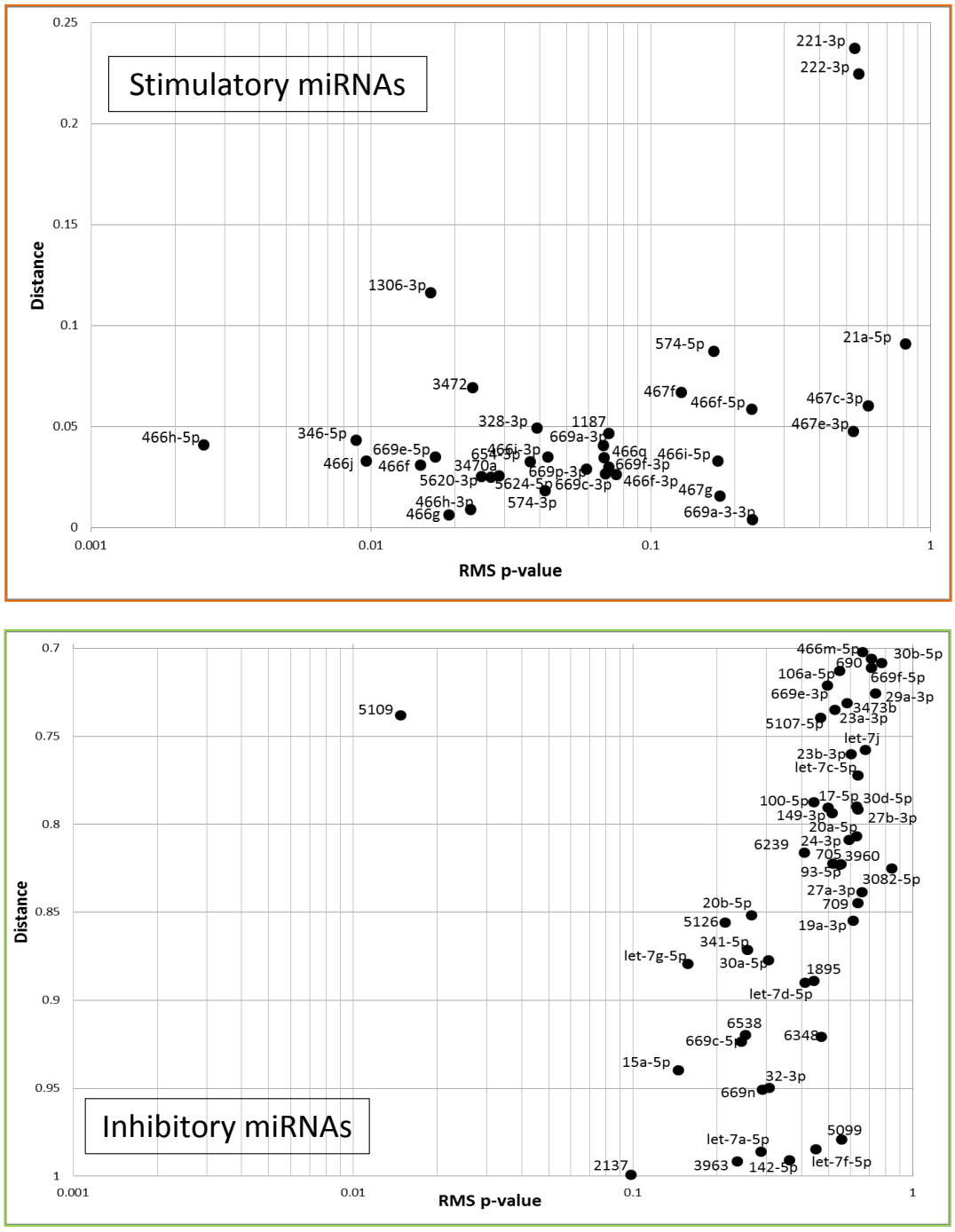

Fig. 3.18. Global identification of stimulatory and inhibitory microRNAs in the distance vs. rms p-value plane. (Top) miRNAs having the same expression pattern as NFATc1 (stimulators). (Bottom) miRNAs having the opposite expression pattern as NFATc1 (inhibitors). Shaded area indicates genes with $p < 0.05$.

3.12 Target Prediction Analysis of the Predicted Regulators

Based on the mechanism of microRNA, stimulator miRNAs were linked to the inhibitory genes and inhibitor miRNAs to the stimulatory genes. Figure 3.19 shows the likeliness of stimulator miRNAs to target inhibitory genes, including eIF2α at various binding energy levels. Figures 3.20 and 3.21 show the likeliness of inhibitor miRNAs to target stimulatory genes, including NFATc1 itself, at various binding energy levels.

Priority of validation will be given to the miRNAs with the most negative energy levels and predicted by the two algorithms.

miRanda / RNA Hybrid	eIF2s1	Agap1	Pacs2	Ttf2	Pla2g15	Tob1	Sgk1	Zfyve21	Cutc	Gins4	Paox	Cbr3	Tnfaip8l2	Ddit4	Usp2	Xbp1	Ypel3	Tpd52
miR-222-3p		-22		-10				-30		-30				-10	-10	-10		-10
miR-221-3p	-10	-26	-10	-10										-10	-10	-10		-10 -26
miR-5620-3p		-22	-10		-30 -36	-10	-30	-10					-10	-36			-10 -30	-10
miR-3472		-10		-30							-26 -33							-24
miR-3095-3p		-24	-26	-10		-10	-22			-22					-10 -30			-22
miR-466h-3p	-33 -36		-26 -36		-24									-26		-30		
miR-669a-3-3p				-10														
miR-669f-3p	-30 -36	-10	-36 -36											-10				-10
miR-466g	-24	-10	-33				-10	-10										
miR-669a-3p	-26		-30	-10														
miR-574-3p		-26					-26				-10	-10			-10 -30			
miR-466i-5p	-10	-36 -39	-10	-10					-26				-10		-26 -33			
miR-574-5p	-10	-39 -39	-24		-30			-10							-30		-30	
miR-669p-3p	-30 -36		-33	-10														
miR-466f-3p	-30 -39	-10	-36 -39						-10					-10		-30		-10
miR-466f-5p		-24							-33	-22					-24 -33			
miR-466q	-30 -36		-30	-10			-10		-10							-10		
miR-3470a	-10	-10						-10							-30	-10		-10
miR-467c-3p	-26					-10												
miR-467g	-30 -33		-30 -33											-10				
miR-669c-3p	-30 -33	-10	-30 -33	-10				-10	-10					-10	-24		-10	
miR-1187	-22	-30	-10			-10					-10				-30 -33		-10	-10
miR-669e-5p	-10	-10	-22	-10		-10		-10		-10	-10				-26			
miR-466f	-22	-26							-26 -33						-30 -33			
miR-466i-3p	-33 -36		-33 -36													-30		
miR-466j									-30 -33						-24 -33			
miR-654-3p											-30							
miR-346-5p		-26					-24	-39	-33		-33	-33			-30 -39	-33	-33	-33
miR-328-3p		-30 -39				-26		-36				-36		-30 -33	-30 -30	-24 -30	-30	-33
miR-466h-5p			-30	-26														
miR-467e-3p	-26					-10												
miR-467f	-30 -33		-30													-30		

Fig. 3.19. Predicted targets and binding energy between stimulatory miRNAs and inhibitory genes. Orange cells are the results obtained by the miRanda algorithm, while the blue cells are obtained by the RNAhybrid algorithm.

miRanda / RNA Hybrid	Nfatc1	Pcdh7	Cd14	Dscr1	Sdc4	Lats1	Myo1e	Adora2b	Ifngr2	Syt16	Itga5	Ppm1l	Egr2	Antxr2	Dusp2	Nfkb1	Slc25a25	Junb	Plaur	Jdp2	Fndc7
miR-20a-5p	-10	-10				-10	-10	-10	-10	-10		-10 -26	-10		-10	-10	-24 -26				
miR-24-3p	-10				-10	-22	-10	-10			-10	-24				-24	-24 -30		-24	-10	-24
miR-93-5p		-10							-10	-10		-24	-10		-10 -26		-10	-22			
miR-142-5p									-10						-10						-10
miR-29a-3p	-24	-10				-10	-10	-10	-10		-24				-10						-10
miR-19a-3p		-10				-10						-10					-10				
miR-30b-5p						-10			-10			-10		-10							
miR-341-5p		-22					-10					-22 -26				-22	-22				
miR-106a-5p		-10				-24			-10	-10	-10		-10		-10		-26 -30				
miR-467d-3p		-10				-10				-10			-10								-10
miR-25-3p	-30					-10					-10	-22	-10	-10		-10					
miR-2137	-36	-33	-30		-26 -33	-39	-36	-36	-33			-22 -33	-36		-30 -39	-36 -41	-39	-26 -41	-36	-36	-30
miR-7a-5p	-24	-10	-10				-10		-10	-10						-10			-10		
miR-23a-3p						-10	-22	-10	-10					-10			-10		-10	-10	
miR-23b-3p							-10	-10	-10								-10		-10	-10	
miR-15a-5p					-10	-10	-22		-22	-10	-22	-10	-10	-10	-10	-10	-10 -26	-10	-10		-10
miR-3963	-10				-10						-10	-10				-10		-10			
miR-17-5p						-22		-10	-10	-10			-10		-10		-26 -30				
miR-30d-5p						-10			-10			-10		-10						-10	
miR-16-5p	-10	-10			-10	-10	-10		-10	-10	-10		-10	-10	-22	-22	-22	-22	-10		-10
miR-30a-5p						-10			-10			-10		-10						-10	
miR-125b-5p												-22 -26		-10		-22	-22				-10
miR-467a-3p	-10					-10					-10				-24			-22			
miR-20b-5p	-10	-22				-10	-10		-10			-10 -26	-10		-10 -30		-22				
miR-5099												-10			-10		-10				-10
miR-18a-5p	-10	-10			-10	-10	-10		-10	-10	-22	-10									
miR-99a-5p												-22									-22
miR-181a-5p		-10			-10		-10	-10			-10			-10			-10			-10	-10
miR-709	-30 -36	-30 -33			-26 -30	-24		-22		-24	-26	-26 -30	-30	-22	-30 -36	-26	-26		-26 -33	-30	-24 -36
miR-15b-5p	-10				-10	-10	-10		-10	-10	-22	-10	-10	-10	-10	-10	-10	-10	-10		-10
miR-27a-3p	-10	-10				-10		-10	-26 -30	-10	-22	-10		-10		-10	-10				-10
miR-27b-3p	-10	-10				-10		-10	-24 -26	-10	-10			-22		-10	-10				-10
miR-103-3p		-10	-10		-10	-10	-10			-10	-10	-10	-10				-26	-10			-10
miR-669e-3p	-10					-10							-10								
miR-106b-5p		-10				-10			-10	-10			-10		-22		-10				
miR-669n						-10		-10			-10	-10		-10							-10
miR-32-3p	-10	-10			-10	-10						-10				-10					
miR-5126	-30 -43	-39	-43		-39	-33 -43	-30 -41	-43	-39 -43	-30 -41	-43	-36 -43	-41	-41	-43	-43 -43	-36 -41	-41 -43	-43	-41	-39
miR-5109		-10	-10			-26	-22			-10						-33				-10	-33
miR-100-5p	-22											-10									-22
miR-19b-3p		-10				-10						-10									
miR-466m-3p		-10			-24	-10				-10	-10	-10	-10		-26 -30			-26			-10
miR-5121						-10						-10	-10				-10				

Fig. 3.20. Predicted targets and binding energy between inhibitory miRNAs and stimulatory genes. Yellow cells are the results obtained by the miRanda algorithm, while the green cells are obtained by the RNAhybrid algorithm.

miRanda RNA Hybrid	Tnip1	Ptpn22	Marcksl 1	Pdgfb	Icam1	Zswim4	Rhoc	Bcl3	Hipk2	Ccnd1	Cdc42ep 4	Traf1	Dhrsx	Frmd6	Wsb2	Plekho2	Ltb	Relb	Irg1	Micall2
miR-20a-5p					-10		-10			-10				-10	-10	-10	-10	-10		
miR-24-3p	-10		-22	-22	-22	-10	-26	-10	-10 -30	-10	-10	-24		-10	-10	-24		-10	-22	-10
miR-93-5p	-30				-10		-10	-33	-10	-24		-10 -26		-10	-10	-10	-10	-10 -30		
miR-142-5p				-10					-10					-10	-10					
miR-29a-3p				-10	-22					-10										-10
miR-19a-3p	-10	-10		-10				-10		-10		-10		-10	-10					
miR-30b-5p	-10	-10							-10						-10	-10				
miR-341-5p	-26			-22	-22		-30	-26		-22			-26			-10		-36 -36		
miR-106a-5p							-10 -26			-10		-10		-10	-10	-10	-10	-10		
miR-467d-3p				-10	-10				-10					-10	-30 -33					
miR-25-3p				-10	-10			-10				-10				-10		-10		
miR-2137	-33		-26 -39	-24	-33	-26 -39	-33	-33	-33	-39	-36	-36	-26 -36	-39	-26 -36	-22 -36	-36	-36	-36	-33
miR-7a-5p		-10				-10				-10		-22		-10	-10	-10		-10		
miR-23a-3p		-10	-10		-10	-22			-10	-10		-10								
miR-23b-3p		-10	-10			-10			-10	-10		-10								
miR-15a-5p		-10		-10	-10	-10		-10	-10	-10	-10	-10	-10				-10		-10	
miR-3963									-10		-10									-10
miR-17-5p					-10		-10 -26			-10		-10		-10	-10	-10		-10		
miR-30d-5p															-10	-10				
miR-16-5p		-10 -26		-10	-10	-26		-10	-10	-10	-10	-10	-10		-10		-10		-10	
miR-30a-5p	-10														-10	-10				
miR-125b-5p		-24			-22	-10					-10	-30	-22				-33		-10	-10
miR-467a-3p				-10	-10				-10					-10	-30 -33					
miR-20b-5p	-30				-22		-10			-10				-10	-10		-10	-10		
miR-5099																				
miR-18a-5p					-10	-10			-10		-10	-10		-10		-10			-10	
miR-99a-5p		-10															-10 -33			
miR-181a-5p					-10							-26	-10		-10			-10	-10	-10
miR-709	-10 -26	-30	-10 -30	-22	-24	-10	-26 -30	-26 -30		-10 -26	-10 -30	-22 -30	-26 -33		-10 -33	-10 -36	-10	-41 -41	-10	-26
miR-15b-5p		-10		-10	-10	-10		-10	-10	-10	-10	-10	-10		-10 -30		-10		-10	
miR-27a-3p	-10			-10	-10		-26		-10				-10	-10	-22			-10	-10	
miR-27b-3p	-10				-10			-10	-10				-10		-10			-10	-10	
miR-103-3p		-10			-26	-10	-10 -30			-22	-10			-24	-30			-10	-22	
miR-669e-3p				-10					-10					-10						
miR-106b-5p					-10		-10			-10		-10		-10	-10	-10	-10	-10		
miR-669n	-10					-10			-10		-10									
miR-32-3p				-10																
miR-5126	-30 -43		-36 -43	-33 -43	-24 -43	-43	-39	-33 -43	-43	-41	-43	-43	-43	-43	-39	-22 -41	-43	-43	-41	-36 -43
miR-5109	-26							-26 -30		-33	-22				-26					
miR-100-5p																	-10 -33			
miR-19b-3p	-10	-10		-10				-10		-10		-10		-10	-10					
miR-466m-3p				-10		-10			-24	-10			-10	-10	-36 -39					
miR-5121					-10	-10			-26											-10

Fig. 3.21. Continuation of predicted targets and binding energy between inhibitory miRNAs and stimulatory genes. Yellow cells are the results obtained by the miRanda algorithm, while the green cells are obtained by the RNAhybrid algorithm.

4. DISCUSSION

Experimental results demonstrated that the differentiation of RAW 264.7 pre-osteoclasts to multi-nucleated osteoclasts was inhibited by the administration of salubrinal and guanabenz, both of which block the dephosphorylation of eIF2α and elevate the level of p-eIF2α. The growth area of the multinucleated cells was reduced by both agents significantly. Partially silencing eIF2α using RNA interference significantly recovered salubrinal- and guanabenz-driven reduction of NFATc1 expression. By evaluating microarray-derived expression of transcription factors, potential regulators involved in salubrinal- and guanabenz-driven regulation of NFATc1 were predicted and evaluated. By considering thermodynamic binding energy of miRNAs to predicted genes, we may also be able to facilitate the selection of miRNAs for further in vitro validation. The results herein suggest that the elevation of p-eIF2α by salubrinal and guanabenz is capable of regulating osteoclastogenesis by targeting NFATc1, and eIF2α mediated signaling may play a significant role not only in osteoblastogenesis but also in osteoclastogenesis.

4.1 Inhibition of Osteoclastogenesis by the Elevation of eIF2α

The results revealed that salubrinal and guanabenz suppresses RANKL–induced osteoclastogenesis through the suppression of its master regulator NFATc1. It has been reported that NFATc1 plays an essential role in osteoclastogenesis. NFATc1-deficient embryonic stem cells fail to differentiate into osteoclasts in response to RANKL and ectopic expression of NFATc1 causes precursors to undergo osteoclast differentiation even in the absence of RANKL [71, 72]. NFATc1 also induces target genes responsible for osteoclast differentiation and function, including OSCAR, TRAP, cathepsin K, c-Src, and integrin αv/β3 [73–75]. Inactivation of NFATc1 by cy-

closporin A (CsA) was reported to attenuate RANKL-mediated pre-osteoclast cell-cell fusion into multinucleated osteoclasts [76]. Our data clearly showed that both salubrinal and guanabenz suppress NFATc1 expression level and reduce the growth area of multinucleated osteoclasts in a dose-dependent manner. The number of TRAP positive cells and the mRNA levels of NFATc1, OSCAR and TRAP were also decreased.

The elevation of p-eIF2α corresponds to the down-regulation of RANKL-induced NFATc1 by salubrinal and guanabenz. In response to various stresses, the level of p-eIF2α is raised and cells undergo either a survival or apoptosis pathway. It was previously observed in osteoblasts that salubrinal's action mimics the induction of a pro-survival program without imposing damaging stresses, which result in the upregulation of ATF4 without inducing apoptosis [65]. Salubrinal- and guanabenz- induced elevation of p-eIF2α also suppresses NFATc1 without any significant changes in cell mortality or relative cell number. Together with siRNA results, where partially silencing eIF2α significantly suppressed the reduction of NFATc1 by salubrinal and guanabenz, eIF2αmediated signaling showed a prominent role in attenuating osteoclastogenesis.

4.2 Possible Involvement of New Regulators

Regulation of NFATc1 by salubrinal and guanabenz-induced phosphorylation of eIF2α however, was not significantly linked to some known early signaling pathways involved in bone remodeling. The MAPK signaling pathway is known to be activated by RANKL-RANK binding which phosphorylates ERK, p38, and JNK, leading to osteoclast differentiation [32]. NF-ϰB plays a critical role in the regulation of the cell cycle, cell adhesion, cytokine production, and cellular processes in macrophages. Osteoclast formation and their functions are mediated by RANKL-induced NF-ϰB activation [77]. Our data showed that the addition of RANKL to RAW 264.7 cells upregulates the level of phosphorylated ERK, p38, and NF-ϰB. However, administration

of salubrinal and guanabenz did not make any detectable change in their expression level at least up to 2 hours. The result indicates that the elevation of p-eIF2α, which results in global translation attenuation, reduced the expression of NFATc1 in the translational level. The result also reveals, however, that the mRNA level of NFATc1 was also reduced in response to salubrinal and guanabenz. Since the expression level of NFATc1 was reduced transcriptionally and partially silencing eIF2α did not recover NFATc1 expression level fully, the results suggest that regulator(s) yet to be identified are involved in the downregulation of NFATc1 by salubrinal and guanabenz.

4.3 Prediction of Stimulators and Inhibitors of NFATc1

The in silico prediction method allows for systematic targeting of potential NFATc1 regulators. One-thousand-twenty-four potential regulators of NFATc1 obtained from genome wide microarray were investigated. The goal was to obtain a group of candidate transcription factors up-stream of NFATc1 which are induced by RANKL and regulated by salubrinal and guanabenz. Four hours was the length of time of treatment chosen due to the observation where the expression level of NFATc1 significantly changed by RANKL at 8 hours of treatment. Therefore, sometime before 8 hours should be appropriate to detect the change in mRNA levels of the regulator candidates. NFATc1 mRNA expressions pattern was used as a base line for the analysis where it is up-regulated by the treatment of RANKL and down-regulated by both salubrinal and guanabenz. The ideal stimulator candidate displays the change in expression pattern similar to that of NFATc1, while the ideal inhibitor candidate displays the change in expression pattern opposite to that of NFATc1.

The two parameters (distance and p-value) facilitated to selecting the candidate stimulators and inhibitors of NFATc1. Distance (between 0 and 1) was determined using Pearson's correlation coefficient, which measures similarity of mRNA expression pattern of a gene of interest to that of NFATc1. The closer the distance to 1, the more similar the expression pattern of the gene is to that of NFATc1. Conversely, the

closer the distance to 0, the more different the expression pattern is. Several methods for selecting candidate regulators were considered before choosing Pearson's correlation. Rank correlation methods, such as Spearman's and Kendall's correlations, are capable of showing whether or not a gene tends to be similar or opposite in pattern to NFATc1. However, they are not able to show whether or not the increase or decrease in expression level is proportional to NFATc1. Euclidian distance was also considered since it could give the measurement of how far a gene's expression level was to NFATc1 expression level. However, the measurement is based strictly on the value of NFATc1 expression level. Applying the root mean square (rms) p-value allows to define representative statistical significance among the four groups of microarray samples. The genes with the most significance and the closest distance were validated using qPCR to confirm their expression patterns. Among them, 6 inhibitory and 6 stimulatory genes were confirmed, creating a smaller pool of gene candidates. Further validation will test whether or not they are upstream of NFATc1.

4.3.1 In Vitro Validation of Zfyve21 and Ddit4 as Inhibitors of NFATc1

Among the 12 qPCR confirmed genes, Zfyve21 and Ddit4 were validated for their upstream involvement in regulating NFATc1 using loss-of-function or siRNA silencing method. Partial knock-down by siRNA of both Zfyve21 and Ddit4 resulted in partial up-regulation of NFATc1 expression level, suggesting their inhibitory role on NFATc1. It is possible, however, that these genes both inhibit and are inhibited by NFATc1. Therefore, further investigation is required to evaluate the possibility of inhibitory feedback involvement instead of upstream inhibition on NFATc1.

It has been reported that Zfyve21 is expressed in most tissues including adherent cell lines, and it regulates the disassembly of focal adhesions (FAs) by promoting the de-phosphorylation of FAK at Tyr397 [78]. However, the role Zfyve21 in osteoclast has not been studied. Studies reported that Ddit4 is induced by a wide variety of stresses, such as hypoxia, oxidative stress, food deprivation, and ER stress [79–82].

Interestingly, a study on hepatocytes showed that Ddit4 is induced by the activation of PERK p-eIF2α ATF4 [82]. It has not been reported, however, whether Ddit4 is induced by p- eIF2α in osteoclasts. Further investigation needs to be done to clarify the role of Ddit4 and Zfyve21 in regulating osteoclast development by salubrinal and guanabenz.

4.3.2 Preliminary Prediction of MicroRNAs

The involvement of microRNA was preliminarily examined by using a similar in silico method to correlate the microRNA array expressions to NFATc1 expressions. Similar to the genes, the microRNAs are categorized into potential stimulators and inhibitors of NFATc1. However, since microRNA binding of the 3' UTR of its target mRNA results in gene silencing, the definition of stimulator and inhibitor for microRNA is different. In the regulation of NFATc1, stimulator microRNAs would ideally silence the genes inhibiting NFATc1 expression. On the other hand, inhibitor microRNAs would silence the genes stimulating NFATc1 or NFATc1 itself. NFATc1 is not the only target gene of interest, and thus all predicted regulators should be taken into count. It is possible that a single microRNA could interact with multiple mRNAs and each of those mRNAs could have multiple microRNA binding sites [84].

A study on the pathogenesis of liver cancer found that Ddit4 is a possible target of miR-221 [85]. In our analysis, miR-221-3p was included as a potential stimulator, and Ddit4 was one of its targets. This example indicates that categorizing the microRNAs using Pearson's method can generate a library of potential stimulatory and inhibitory microRNAs that could interact with the predicted target genes. Current analysis using Pearson's method alone may not be sufficient, and further analysis is recommended to identify the role of microRNAs in salubrinal- and guanabenz-driven regulation of NFATc1.

We also employed an online integrated tool, "miRNA_targets", which implements two miRNA analysis algorithms that provide prediction of target sites based on their

thermodynamic binding stability. Both algorithms used full length mRNAs instead of relying on 3' UTR regions, which includes 5'-region as well as the coding regions and is not restricted to the seed region and experimentally validated miRNA. This makes it possible to examine a wider set of potential target genes. Constructing a table that lists a set of miRNAs and their target genes facilitates in silico analysis and is useful for selecting microRNAs for future in vitro validation. For example, after a gene is validated and confirmed to regulate NFATc1, its potential miRNA candidates could be chosen based on the prediction from binding energy stability. Then, those candidates could be qPCR validated in the order from most significant (p_i value) and closest distance (d_i value) to the least.

4.4 Future Studies

The prediction results may lead to future research directions in vitro, in vivo, and in silico. First, more microarray data could be obtained from samples treated with NFATc1 siRNA which would be an aid in selecting genes upstream of NFATc1. Obtaining a microarray data from samples treated with eIF2α siRNA could also be useful as an aid in selecting genes with downstream involvement of eIF2α. Second, more prediction result for microRNA could be obtained from other algorithms that use different criteria for its prediction. The current result is based on thermodynamic binding stability only and other criteria such as complete seed pairing, conservation in related species, and multiple target binding sites, could strengthen the prediction result. Third, gain-of-function by plasmid overexpression could be used following the loss-of-function by siRNA to further confirm the regulators involvement in regulating NFATc1. After the role of candidate regulators of interest is validated by these functional assays, examining a phenotype of knockout mice could be the next logical step.

5. CONCLUSIONS

Using in vitro experimental methods, administration of salubrinal and guanabenz was shown to inhibit the differentiation of RAW 264.7 pre-osteoclasts to multi-nucleated osteoclasts through the downregulation of NFATc1 without inducing apoptosis. The results also support the involvement of eIF2α signaling in the regulation of NFATc1 by salubrinal and guanabenz. Some of the known signaling pathways for osteoclastogenesis were not affected by the administration of salubrinal and guanabenz, and an in silico microarray-evaluation method was conducted to predict the potential involvement of other signaling pathways. The generated informative graphs were able to direct our focus towards an efficient and selective gene validation. Preliminary in silico microRNA results will be useful for future guidance in discovering the involvement of microRNA in salubrinal- and guanabenz-driven regulation of NFATc1.

In summary, the results in this thesis demonstrate that salubrinal and guanabenz are capable of attenuating osteoclastogenesis through the suppression of NFATc1 through eIF2α signaling and other signaling pathway(s). The latter might be driven by transcription factor(s) and microRNA(s), which have not been identified as a regulator of osteoclastogenesis. Together with the previous study on osteoblasts, the results in this thesis suggest that salubrinal and guanabenz are able to regulate the development of both osteoblasts and osteoclasts. Currently, no therapeutic agent for osteoporosis is based on eIF2α signaling and no drugs regulate development of osteoblasts as well as osteoclasts. Although further study and analysis are recommended to further identify the mechanism of action of eIF2α-mediated signaling in bone remodeling, this thesis supports a possibility of developing a novel synthetic drug for treatment and care of those suffering from osteoporosis.

LIST OF REFERENCES

LIST OF REFERENCES

[1] S. C. Manolagas and R. L. Jilka, "Bone marrow, cytokines, and bone remodeling. emerging insights into the pathophysiology of osteoporosis.," *The New England journal of medicine*, vol. 332, no. 5, pp. 305–311, 1995.

[2] A. Parfitt, "Osteonal and hemi-osteonal remodeling: The spatial and temporal framework for signal traffic in adult human bone," *Journal of cellular biochemistry*, vol. 55, no. 3, pp. 273–286, 1994.

[3] S. C. Miller and W. S. Jee, "The bone lining cell: a distinct phenotype?," *Calcified tissue international*, vol. 41, no. 1, pp. 1–5, 1987.

[4] L. A. Armas and R. R. Recker, "Pathophysiology of osteoporosis new mechanistic insights," *Endocrinology and metabolism clinics of North America*, vol. 41, no. 3, 2012.

[5] F. Vescini and F. Grimaldi, "Pth 1–84: bone rebuilding as a target for the therapy of severe osteoporosis," *Clinical Cases in Mineral and Bone Metabolism*, vol. 9, no. 1, p. 31, 2012.

[6] D. W. Dempster, C. L. Lambing, P. J. Kostenuik, and A. Grauer, "Role of rank ligand and denosumab, a targeted rank ligand inhibitor, in bone health and osteoporosis: a review of preclinical and clinical data," *Clinical therapeutics*, vol. 34, no. 3, pp. 521–536, 2012.

[7] J. Gallagher, D. Goldgar, and A. Moy, "Total bone calcium in normal women: effect of age and menopause status," *Journal of bone and mineral research*, vol. 2, no. 6, pp. 491–496, 1987.

[8] R. P. Heaney, "Estrogen-calcium interactions in the postmenopause: a quantitative description," *Bone and mineral*, vol. 11, no. 1, pp. 67–84, 1990.

[9] B. Nordin, A. Need, A. Bridges, and M. Horowitz, "Relative contributions of years since menopause, age, and weight to vertebral density in postmenopausal women.," *Journal of Clinical Endocrinology & Metabolism*, vol. 74, no. 1, pp. 20–23, 1992.

[10] R. Eastell, P. D. DELMAS, S. F. HODGSON, E. F. ERIKSEN, K. G. MANN, and B. L. RIGGS, "Bone formation rate in older normal women: concurrent assessment with bone histomorphometry, calcium kinetics, and biochemical markers," *Journal of Clinical Endocrinology & Metabolism*, vol. 67, no. 4, pp. 741–748, 1988.

[11] O. Johnell and J. Kanis, "An estimate of the worldwide prevalence and disability associated with osteoporotic fractures," *Osteoporosis International*, vol. 17, no. 12, pp. 1726–1733, 2006.

[12] X. Wu, S. Guo, X. Ma, G. Shen, C. Yang, K. Xie, J. Liu, W. Guo, Y. Yan, and E. Luo, "Screening of osteoprotegerin-related feature genes in osteoporosis and functional analysis with dna microarray," *European journal of medical research*, vol. 18, no. 1, p. 15, 2013.

[13] S. Blume and J. Curtis, "Medical costs of osteoporosis in the elderly medicare population," *Osteoporosis International*, vol. 22, no. 6, pp. 1835–1844, 2011.

[14] A. Parfitt, "The two-stage concept of bone loss revisited," *Triangle*, vol. 31, pp. 99–110, 1992.

[15] A. Parfitt, "Bone-forming cells in clinical conditions," *Bone*, vol. 1, pp. 351–429, 1990.

[16] E. F. Eriksen, S. F. Hodgson, R. Eastell, B. L. RIGGS, S. L. Cedel, and W. M. O'Fallon, "Cancellous bone remodeling in type i (postmenopausal) osteoporosis: quantitative assessment of rates of formation, resorption, and bone loss at tissue and cellular levels," *Journal of Bone and Mineral Research*, vol. 5, no. 4, pp. 311–319, 1990.

[17] Q. Yang, J. Jian, S. B. Abramson, and X. Huang, "Inhibitory effects of iron on bone morphogenetic protein 2–induced osteoblastogenesis," *Journal of Bone and Mineral Research*, vol. 26, no. 6, pp. 1188–1196, 2011.

[18] M. N. Weitzmann, R. Pacifici, *et al.*, "Estrogen deficiency and bone loss: an inflammatory tale," *Journal of Clinical Investigation*, vol. 116, no. 5, pp. 1186–1194, 2006.

[19] T. Shibata, A. Shira-Ishi, T. Sato, T. Masaki, A. Sasaki, Y. Masuda, A. Hishiya, N. Ishikura, S. Higashi, Y. Uchida, *et al.*, "Vitamin d hormone inhibits osteoclastogenesis in vivo by decreasing the pool of osteoclast precursors in bone marrow," *Journal of Bone and Mineral Research*, vol. 17, no. 4, pp. 622–629, 2002.

[20] A. Cranney, T. Horsley, S. O'Donnell, H. Weiler, L. Puil, D. Ooi, S. Atkinson, L. Ward, D. Moher, D. Hanley, *et al.*, "Effectiveness and safety of vitamin d in relation to bone health," 2007.

[21] H. A. Bischoff-Ferrari, W. C. Willett, E. J. Orav, P. Lips, P. J. Meunier, R. A. Lyons, L. Flicker, J. Wark, R. D. Jackson, J. A. Cauley, *et al.*, "A pooled analysis of vitamin d dose requirements for fracture prevention," *New England Journal of Medicine*, vol. 367, no. 1, pp. 40–49, 2012.

[22] G. Jones, "Vitamin d and analogues," *Principles of bone biology. Third edition. Section: pharmacological mechanisms of therapeutics, Academic Press Inc, San Diego (CA)*, pp. 1777–1799, 2008.

[23] V. A. Moyer, "Vitamin d and calcium supplementation to prevent fractures in adults: Us preventive services task force recommendation statement," *Annals of Internal Medicine*, 2013.

[24] I. R. Reid and M. J. Bolland, "Calcium supplements: bad for the heart?," *Heart*, vol. 98, no. 12, pp. 895–896, 2012.

[25] I. Persson, "Cancer risk in women receiving estrogen-progestin replacement therapy," *Maturitas*, vol. 23, pp. S37–S45, 1996.

[26] B. L. Riggs, S. Khosla, and L. J. Melton, "Sex steroids and the construction and conservation of the adult skeleton," *Endocrine reviews*, vol. 23, no. 3, pp. 279–302, 2002.

[27] J. Alexander, I. Bab, S. Fish, R. Müller, T. Uchiyama, G. Gronowicz, M. Nahounou, Q. Zhao, D. White, M. Chorev, *et al.*, "Human parathyroid hormone 1–34 reverses bone loss in ovariectomized mice," *Journal of Bone and Mineral Research*, vol. 16, no. 9, pp. 1665–1673, 2001.

[28] C. J. Rosen and J. P. Bilezikian, "Anabolic therapy for osteoporosis," *Journal of Clinical Endocrinology & Metabolism*, vol. 86, no. 3, pp. 957–964, 2001.

[29] D. M. Black, S. R. Cummings, D. B. Karpf, J. A. Cauley, D. E. Thompson, M. C. Nevitt, D. C. Bauer, H. K. Genant, W. L. Haskell, R. Marcus, *et al.*, "Randomised trial of effect of alendronate on risk of fracture in women with existing vertebral fractures," *The Lancet*, vol. 348, no. 9041, pp. 1535–1541, 1996.

[30] S. R. Cummings, J. S. Martin, M. R. McClung, E. S. Siris, R. Eastell, I. R. Reid, P. Delmas, H. B. Zoog, M. Austin, A. Wang, *et al.*, "Denosumab for prevention of fractures in postmenopausal women with osteoporosis," *New England Journal of Medicine*, vol. 361, no. 8, pp. 756–765, 2009.

[31] J.-J. Body, P. Bergmann, S. Boonen, J.-P. Devogelaer, E. Gielen, S. Goemaere, J.-M. Kaufman, S. Rozenberg, and J.-Y. Reginster, "Extraskeletal benefits and risks of calcium, vitamin d and anti-osteoporosis medications," *Osteoporosis International*, vol. 23, no. 1, pp. 1–23, 2012.

[32] H. Yasuda, N. Shima, N. Nakagawa, K. Yamaguchi, M. Kinosaki, S.-i. Mochizuki, A. Tomoyasu, K. Yano, M. Goto, A. Murakami, *et al.*, "Osteoclast differentiation factor is a ligand for osteoprotegerin/osteoclastogenesis-inhibitory factor and is identical to trance/rankl," *Proceedings of the National Academy of Sciences*, vol. 95, no. 7, pp. 3597–3602, 1998.

[33] D. Lacey, E. Timms, H.-L. Tan, M. Kelley, C. Dunstan, T. Burgess, R. Elliott, A. Colombero, G. Elliott, S. Scully, *et al.*, "Osteoprotegerin ligand is a cytokine that regulates osteoclast differentiation and activation," *Cell*, vol. 93, no. 2, pp. 165–176, 1998.

[34] E. Canalis, "New treatment modalities in osteoporosis," *Endocrine Practice*, vol. 16, no. 5, pp. 855–863, 2010.

[35] D. Dickson, O. Hargie, and N. Morrow, *Communication skills training for health professionals*. Nelson Thornes, 1996.

[36] H. Fleisch, "Bisphosphonates: mechanisms of action," *Advances in Organ Biology*, vol. 5, pp. 835–850, 1998.

[37] Z. Janovská, "Bisphosphonate-related osteonecrosis of the jaws. a severe side effect of bisphosphonate therapy.," *Acta medica (Hradec Králové)/Universitas Carolina, Facultas Medica Hradec Králové*, vol. 55, no. 3, p. 111, 2012.

[38] S. Khosla, J. P. Bilezikian, D. W. Dempster, E. M. Lewiecki, P. D. Miller, R. M. Neer, R. R. Recker, E. Shane, D. Shoback, and J. T. Potts, "Benefits and risks of bisphosphonate therapy for osteoporosis," *Journal of Clinical Endocrinology & Metabolism*, vol. 97, no. 7, pp. 2272–2282, 2012.

[39] M. T. Drake, B. L. Clarke, and S. Khosla, "Bisphosphonates: mechanism of action and role in clinical practice," in *Mayo Clinic Proceedings*, vol. 83, pp. 1032–1045, Elsevier, 2008.

[40] I. Novoa, Y. Zhang, H. Zeng, R. Jungreis, H. P. Harding, and D. Ron, "Stress-induced gene expression requires programmed recovery from translational repression," *The EMBO journal*, vol. 22, no. 5, pp. 1180–1187, 2003.

[41] P. Tsaytler, H. P. Harding, D. Ron, and A. Bertolotti, "Selective inhibition of a regulatory subunit of protein phosphatase 1 restores proteostasis," *Science Signaling*, vol. 332, no. 6025, p. 91, 2011.

[42] H. P. Harding, I. Novoa, Y. Zhang, H. Zeng, R. Wek, M. Schapira, and D. Ron, "Regulated translation initiation controls stress-induced gene expression in mammalian cells," *Molecular cell*, vol. 6, no. 5, pp. 1099–1108, 2000.

[43] R. F. Riedel, N. Larrier, L. Dodd, S. Martinez, and B. E. Brigman, "The clinical management of chondrosarcoma," *Current treatment options in oncology*, vol. 10, no. 1-2, pp. 94–106, 2009.

[44] M. Brada, M. Pijls-Johannesma, and D. De Ruysscher, "Proton therapy in clinical practice: current clinical evidence," *Journal of clinical oncology*, vol. 25, no. 8, pp. 965–970, 2007.

[45] X.-Z. Wang, H. P. Harding, Y. Zhang, E. M. Jolicoeur, M. Kuroda, and D. Ron, "Cloning of mammalian ire1 reveals diversity in the er stress responses," *The EMBO journal*, vol. 17, no. 19, pp. 5708–5717, 1998.

[46] S. J. Marciniak, C. Y. Yun, S. Oyadomari, I. Novoa, Y. Zhang, R. Jungreis, K. Nagata, H. P. Harding, and D. Ron, "Chop induces death by promoting protein synthesis and oxidation in the stressed endoplasmic reticulum," *Genes & development*, vol. 18, no. 24, pp. 3066–3077, 2004.

[47] B. Song, D. Scheuner, D. Ron, S. Pennathur, and R. J. Kaufman, "Chop deletion reduces oxidative stress, improves β cell function, and promotes cell survival in multiple mouse models of diabetes," *The Journal of clinical investigation*, vol. 118, no. 10, p. 3378, 2008.

[48] K. Y. Tsang, D. Chan, J. F. Bateman, and K. S. Cheah, "In vivo cellular adaptation to er stress: survival strategies with double-edged consequences," *Journal of cell science*, vol. 123, no. 13, pp. 2145–2154, 2010.

[49] M. Boyce, K. F. Bryant, C. Jousse, K. Long, H. P. Harding, D. Scheuner, R. J. Kaufman, D. Ma, D. M. Coen, D. Ron, *et al.*, "A selective inhibitor of eif2α dephosphorylation protects cells from er stress," *Science Signaling*, vol. 307, no. 5711, p. 935, 2005.

[50] V. Subbiah and R. Kurzrock, "Phase 1 clinical trials for sarcomas: the cutting edge," *Current opinion in oncology*, vol. 23, no. 4, pp. 352–360, 2011.

[51] T. Yuan, B.-l. Luo, T.-h. Wei, L. Zhang, B.-m. He, and R.-c. Niu, "Salubrinal protects against cigarette smoke extract-induced hbepc apoptosis likely via regulation of the perk-eif2α signaling pathway," *Archives of medical research*, 2012.

[52] T. Gong, Q. Wang, Z. Lin, M.-l. Chen, and G.-z. Sun, "Endoplasmic reticulum (er) stress inhibitor salubrinal protects against ceramide-induced sh-sy5y cell death," *Biochemical and Biophysical Research Communications*, 2012.

[53] H. C. Drexler, "Synergistic apoptosis induction in leukemic cells by the phosphatase inhibitor salubrinal and proteasome inhibitors," *PloS one*, vol. 4, no. 1, p. e4161, 2009.

[54] M. Koizumi, N. G. Tanjung, A. Chen, J. R. Dynlacht, J. Garrett, Y. Yoshioka, K. Ogawa, T. Teshima, and H. Yokota, "Administration of salubrinal enhances radiation-induced cell death of sw1353 chondrosarcoma cells," *Anticancer Research*, vol. 32, no. 9, pp. 3667–3673, 2012.

[55] S. J. Sequeira, H. C. Wen, A. Avivar-Valderas, E. F. Farias, and J. A. Aguirre-Ghiso, "Inhibition of eif2α dephosphorylation inhibits erbb2-induced deregulation of mammary acinar morphogenesis," *BMC cell biology*, vol. 10, no. 1, p. 64, 2009.

[56] A. C. Ranganathan, S. Ojha, A. Kourtidis, D. S. Conklin, and J. A. Aguirre-Ghiso, "Dual function of pancreatic endoplasmic reticulum kinase in tumor cell growth arrest and survival," *Cancer research*, vol. 68, no. 9, pp. 3260–3268, 2008.

[57] D. M. Schewe and J. A. Aguirre-Ghiso, "Inhibition of eif2α dephosphorylation maximizes bortezomib efficiency and eliminates quiescent multiple myeloma cells surviving proteasome inhibitor therapy," *Cancer research*, vol. 69, no. 4, pp. 1545–1552, 2009.

[58] C. M. Shearer and N. J. Deangelis, "Guanabenz degradation products and stability assay," *Journal of Pharmaceutical Sciences*, vol. 68, no. 8, pp. 1010–1012, 1979.

[59] A. Mockel, C. Obringer, T. B. Hakvoort, M. Seeliger, W. H. Lamers, C. Stoetzel, H. Dollfus, and V. Marion, "Pharmacological modulation of the retinal unfolded protein response in bardet-biedl syndrome reduces apoptosis and preserves light detection ability," *Journal of Biological Chemistry*, vol. 287, no. 44, pp. 37483–37494, 2012.

[60] S.-i. Hino, S. Kondo, K. Yoshinaga, A. Saito, T. Murakami, S. Kanemoto, H. Sekiya, K. Chihara, Y. Aikawa, H. Hara, *et al.*, "Regulation of er molecular chaperone prevents bone loss in a murine model for osteoporosis," *Journal of bone and mineral metabolism*, vol. 28, no. 2, pp. 131–138, 2010.

[61] J. Liu, N. Hoppman, J. R. O'Connell, H. Wang, E. A. Streeten, J. C. McLenithan, B. D. Mitchell, and A. R. Shuldiner, "A functional haplotype in eif2ak3, an er stress sensor, is associated with lower bone mineral density," *Journal of Bone and Mineral Research*, vol. 27, no. 2, pp. 331–341, 2012.

[62] X. Yang, K. Matsuda, P. Bialek, S. Jacquot, H. C. Masuoka, T. Schinke, L. Li, S. Brancorsini, P. Sassone-Corsi, T. M. Townes, *et al.*, "Atf4 is a substrate of rsk2 and an essential regulator of osteoblast biology: implication for coffin-lowry syndrome," *Cell*, vol. 117, no. 3, pp. 387–398, 2004.

[63] T. Murakami, A. Saito, S.-i. Hino, S. Kondo, S. Kanemoto, K. Chihara, H. Sekiya, K. Tsumagari, K. Ochiai, K. Yoshinaga, *et al.*, "Signalling mediated by the endoplasmic reticulum stress transducer oasis is involved in bone formation," *Nature Cell Biology*, vol. 11, no. 10, pp. 1205–1211, 2009.

[64] A. Saito, K. Ochiai, S. Kondo, K. Tsumagari, T. Murakami, D. R. Cavener, and K. Imaizumi, "Endoplasmic reticulum stress response mediated by the perk-eif2α-atf4 pathway is involved in osteoblast differentiation induced by bmp2," *Journal of Biological Chemistry*, vol. 286, no. 6, pp. 4809–4818, 2011.

[65] K. Hamamura, N. Tanjung, and H. Yokota, "Suppression of osteoclastogenesis through phosphorylation of eukaryotic translation initiation factor 2 alpha," *Journal of bone and mineral metabolism*, pp. 1–11, 2013.

[66] P. Zhang, K. Hamamura, C. Jiang, L. Zhao, and H. Yokota, "Salubrinal promotes healing of surgical wounds in rat femurs," *Journal of bone and mineral metabolism*, vol. 30, no. 5, pp. 568–579, 2012.

[67] K. Hamamura and H. Yokota, "Stress to endoplasmic reticulum of mouse osteoblasts induces apoptosis and transcriptional activation for bone remodeling," *FEBS letters*, vol. 581, no. 9, pp. 1769–1774, 2007.

[68] H. Yokota, K. Hamamura, A. Chen, T. R. Dodge, N. Tanjung, A. Abedinpoor, and P. Zhang, "Effects of salubrinal on development of osteoclasts and osteoblasts from bone marrow-derived cells," *BMC musculoskeletal disorders*, vol. 14, no. 1, p. 197, 2013.

[69] X. Huang, Y. Chen, H. Zhang, Q. Ma, Y.-w. Zhang, and H. Xu, "Salubrinal attenuates β-amyloid-induced neuronal death and microglial activation by inhibition of the nf-κb pathway," *Neurobiology of aging*, vol. 33, no. 5, pp. 1007–e9, 2012.

[70] H. Min and S. Yoon, "Got target?: computational methods for microrna target prediction and their extension," *Experimental & molecular medicine*, vol. 42, no. 4, pp. 233–244, 2010.

[71] H. Takayanagi, S. Kim, T. Koga, H. Nishina, M. Isshiki, H. Yoshida, A. Saiura, M. Isobe, T. Yokochi, J.-i. Inoue, *et al.*, "Induction and activation of the transcription factor nfatc1 (nfat2) integrate rankl signaling in terminal differentiation of osteoclasts," *Developmental cell*, vol. 3, no. 6, pp. 889–901, 2002.

[72] H. Hirotani, N. A. Tuohy, J.-T. Woo, P. H. Stern, and N. A. Clipstone, "The calcineurin/nuclear factor of activated t cells signaling pathway regulates osteoclastogenesis in raw264. 7 cells," *Journal of Biological Chemistry*, vol. 279, no. 14, pp. 13984–13992, 2004.

[73] T. N. Crotti, M. Flannery, N. C. Walsh, J. D. Fleming, S. R. Goldring, and K. P. McHugh, "Nfatc1 regulation of the human β¡ sub¿ 3¡/sub¿ integrin promoter in osteoclast differentiation," *Gene*, vol. 372, pp. 92–102, 2006.

[74] F. Ikeda, R. Nishimura, T. Matsubara, K. Hata, S. V. Reddy, and T. Yoneda, "Activation of nfat signal in vivo leads to osteopenia associated with increased osteoclastogenesis and bone-resorbing activity," *The Journal of Immunology*, vol. 177, no. 4, pp. 2384–2390, 2006.

[75] M. Matsumoto, M. Kogawa, S. Wada, H. Takayanagi, M. Tsujimoto, S. Katayama, K. Hisatake, and Y. Nogi, "Essential role of p38 mitogen-activated protein kinase in cathepsin K gene expression during osteoclastogenesis through association of NFATc1 and PU.1," *Journal of Biological Chemistry*, vol. 279, no. 44, pp. 45969–45979, 2004.

[76] K. Kim, S.-H. Lee, J. H. Kim, Y. Choi, and N. Kim, "Nfatc1 induces osteoclast fusion via up-regulation of atp6v0d2 and the dendritic cell-specific transmembrane protein (dc-stamp)," *Molecular Endocrinology*, vol. 22, no. 1, pp. 176–185, 2008.

[77] M. J. Bossard, T. A. Tomaszek, M. A. Levy, C. F. Ijames, M. J. Huddleston, J. Briand, S. Thompson, S. Halpert, D. F. Veber, S. A. Carr, *et al.*, "Mechanism of inhibition of cathepsin k by potent, selective 1, 5-diacylcarbohydrazides: a new class of mechanism-based inhibitors of thiol proteases," *Biochemistry*, vol. 38, no. 48, pp. 15893–15902, 1999.

[78] M. Nagano, D. Hoshino, T. Sakamoto, N. Kawasaki, N. Koshikawa, and M. Seiki, "Zf21 protein regulates cell adhesion and motility," *Journal of Biological Chemistry*, vol. 285, no. 27, pp. 21013–21022, 2010.

[79] J. Brugarolas, K. Lei, R. L. Hurley, B. D. Manning, J. H. Reiling, E. Hafen, L. A. Witters, L. W. Ellisen, and W. G. Kaelin, "Regulation of mTOR function in response to hypoxia by REDD1 and the TSC1/TSC2 tumor suppressor complex," *Genes & development*, vol. 18, no. 23, pp. 2893–2904, 2004.

[80] L. W. Ellisen, K. D. Ramsayer, C. M. Johannessen, A. Yang, H. Beppu, K. Minda, J. D. Oliner, F. McKeon, and D. A. Haber, "REDD1, a developmentally regulated transcriptional target of p63 and p53, links p63 to regulation of reactive oxygen species," *Molecular cell*, vol. 10, no. 5, pp. 995–1005, 2002.

[81] N. K. McGhee, L. S. Jefferson, and S. R. Kimball, "Elevated corticosterone associated with food deprivation upregulates expression in rat skeletal muscle of the mtorc1 repressor, redd1," *The Journal of nutrition*, vol. 139, no. 5, pp. 828–834, 2009.

[82] S. R. Kimball and L. S. Jefferson, "Induction of redd1 gene expression in the liver in response to endoplasmic reticulum stress is mediated through a perk, eif2α phosphorylation, atf4-dependent cascade," *Biochemical and Biophysical Research Communications*, 2012.

[83] U. Ozcan, L. Ozcan, E. Yilmaz, K. Düvel, M. Sahin, B. D. Manning, and G. S. Hotamisligil, "Loss of the tuberous sclerosis complex tumor suppressors triggers the unfolded protein response to regulate insulin signaling and apoptosis," *Molecular cell*, vol. 29, no. 5, pp. 541–551, 2008.

[84] J. B. Lian, G. S. Stein, A. J. Van Wijnen, J. L. Stein, M. Q. Hassan, T. Gaur, and Y. Zhang, "Microrna control of bone formation and homeostasis," *Nature Reviews Endocrinology*, vol. 8, no. 4, pp. 212–227, 2012.

[85] P. Pineau, S. Volinia, K. McJunkin, A. Marchio, C. Battiston, B. Terris, V. Mazzaferro, S. W. Lowe, C. M. Croce, and A. Dejean, "mir-221 overexpression contributes to liver tumorigenesis," *Proceedings of the National Academy of Sciences*, vol. 107, no. 1, pp. 264–269, 2010.

[86] A. B. Chen, K. Hamamura, G. Wang, W. Xing, S. Mohan, H. Yokota, and Y. Liu, "Model-based comparative prediction of transcription-factor binding motifs in anabolic responses in bone," *Genomics, Proteomics & Bioinformatics*, vol. 5, no. 3, pp. 158–165, 2007.

APPENDICES

APPENDICES: MATLAB SOURCE CODE

The appendices include two categories of MATLAB source code: one to predict gene regulators and the other to predict microRNA regulators that potentially regulate NFATc1. The programs were run using MATLAB R2010a software. The input of the programs were the microarray-derived data, including feature names, signal values, fold change values, and p-values. The programs output a list of predicted genes and microRNAs potentially regulating NFATc1 along with a distance (d_i) and RMS p-value (p_i), ordered by distance from NFATc1 expression pattern.

A Prediction of Potential Gene Regulators

The code for "Gene Screening" and "Gene Distance and P-value" are included in this category. The purpose of the "Gene Screening" code is to filter the microarray data and divide the genes into two groups: stimulatory and inhibitory genes. This program takes the names, signal values, fold change values, and p-values 1025 genes as input. It outputs genes with stimulatory and inhibitory characteristics. The procedure has four sections. First, the microarray data is imported and each column was put into individual arrays. Second, the duplicated genes are removed, and the remaining genes are filtered based on fold change criteria. Third, the genes are divided into stimulatory and inhibitory groups. Fourth, the output is written to an Excel file with one sheet of stimulatory genes and one sheet of inhibitory genes.

The purpose of the "Gene Distance and P-value" code is to calculate the distance and p-value of each gene using Pearson's correlation method and RMS, respectively. The inputs are the names, signal values, and p-values of the stimulatory and inhibitory genes from "Gene Screening" result. NFATc1 signal values are also used to calculate each gene's distance from NFATc1 expression pattern. The output of this program

would be the calculated distance (d_i) and p-value (p_i) of each gene. The procedure includes five sections. First, the stimulatory and inhibitory gene data are imported, and each column was put into individual arrays. Second, the mean signal value of each treatment category is calculated for each gene. Third, the distance (d_i) of each gene is calculated using Pearson's correlation method. Fourth, the p-value of each gene is calculated using RMS. Fifth, the gene names, distance, and p-value are written into an Excel file ordered by distance.

A.1 Gene Screening

```
clear, clc

%Matlab input: names, fold change, pvalue, signal values of genes
file = 'genematlabnormalized.xlsx';

%ONE: importing data into individual arrays

%Control (C) and RANKL (R) treatments
[numR stringR] = xlsread(file,1);
Rname = stringR(3:end,1);
RFC = numR(:,2);
RlogFC = numR(:,3);
Rpval = numR (:,4);
Rdef = stringR (3:end,5);
Racc = stringR(3:end,6);
R1 = numR(:,7);
R2 = numR(:,8);
R3 = numR(:,9);
C1 = numR(:,10);
C2 = numR(:,11);
```

```
C3 = numR(:,12);
%RANKL+salubrinal (S) treatment
[numS stringS] = xlsread(file,2);
Sname = stringS(3:end,1);
SFC = numS(:,2);
SlogFC = numS(:,3);
Spval = numS (:,4);
S1 = numS(:,5);
S2 = numS(:,6);
S3 = numS(:,7);
%RANKL+guanabenz (G) treatment
[numG stringG] = xlsread(file,3);
Gname = stringG(3:end,1);
GFC = numG(:,2);
GlogFC = numG(:,3);
Gpval = numG (:,4);
G1 = numG(:,5);
G2 = numG(:,6);
G3 = numG(:,7);



%TWO: removing duplicates and filtering based on fold change
    values


%control and RANKL treatment
[Rname a] = unique (Rname); %removing duplicates
RFC = RFC(a);
RlogFC = RlogFC(a);
Rpval = Rpval(a);
Rdef = Rdef(a);
Racc = Racc(a);
```

```
R1 = R1(a);
R2 = R2(a);
R3 = R3(a);
C1 = C1(a);
C2 = C2(a);
C3 = C3(a);
%eliminates genes if fold change is -1.1<0<1.1
a = find ( ((RFC > 1.1) + (RFC < -1.1)) >= 1);
Rname = Rname(a);
RFC = RFC(a);
RlogFC = RlogFC(a);
Rpval = Rpval(a);
Rdef = Rdef(a);
Racc = Racc(a);
R1 = R1(a);
R2 = R2(a);
R3 = R3(a);
C1 = C1(a);
C2 = C2(a);
C3 = C3(a);
%salubrinal treatment
[Sname b] = unique (Sname); %removing duplicates
SFC = SFC(b);
SlogFC = SlogFC(b);
Spval = Spval(b);
S1 = S1(b);
S2 = S2(b);
S3 = S3(b);
%eliminates genes if fold change is -1.1<0<1.1
b = find ( ((SFC > 1.1) + (SFC < -1.1)) >= 1);
Sname = Sname(b);
```

```
SFC = SFC(b);
SlogFC = SlogFC(b);
Spval = Spval(b);
S1 = S1(b);
S2 = S2(b);
S3 = S3(b);
%guanabenz treatment
[Gname c] = unique (Gname); %removing duplicates
GFC = GFC(c);
GlogFC = GlogFC(c);
Gpval = Gpval(c);
G1 = G1(c);
G2 = G2(c);
G3 = G3(c);
%eliminates genes if fold change is -1.1<0<1.1
c = find ( ((GFC > 1.1) + (GFC < -1.1)) >= 1);
Gname = Gname(c);
GFC = GFC(c);
GlogFC = GlogFC(c);
Gpval = Gpval(c);
G1 = G1(c);
G2 = G2(c);
G3 = G3(c);


%counting the length of list from each treatment category
l1 = length(Rname); %RANKL treatment
l2 = length(Sname); %salubrinal treatment
l3 = length(Gname); %guanabenz treatment
similar_neg = [];
similar_pos = [];
threesim = [];
```

```
threesim_neg = [];
threesim_pos = [];
similar = [];


%THREE: Putting into stimulatory and inhibitory groups

%Find common genes in salubrinal and guanabenz treatments
for i1 = 1:l2,
    for i2 = 1:l3,
        if strcmp(Sname(i1), Gname(i2)),
            similar = [similar; Sname(i1) SFC(i1) Spval(i1)
               SlogFC(i1) GFC(i2) Gpval(i2) GlogFC(i2) S1(i1) S2(
               i1) S3(i1) G1(i2) G2(i2) G3(i2)];
             if ( SFC(i1) < 0 && GFC(i2) <0),
                 similar_neg = [similar_neg; Sname(i1) SFC(i1)
                    Spval(i1) SlogFC(i1) GFC(i2) Gpval(i2) GlogFC
                    (i2)];
             elseif (SFC(i1) >0 && GFC(i2) >0),
                similar_pos = [similar_pos; Sname(i1) SFC(i1)
                   Spval(i1) SlogFC(i1) GFC(i2) Gpval(i2) GlogFC(
                   i2)];
             end
        end
    end
end

twosimSname = similar(:,1);
twosimSFC = cell2mat(similar(:,2));
twosimSpval = similar(:,3);
twosimSlogFC = similar(:,4);
```

```
twosimGFC = cell2mat(similar(:,5));
twosimGpval = similar(:,6);
twosimGlogFC = similar(:,7);
SS1 = similar(:,8);
SS2 = similar(:,9);
SS3 = similar(:,10);
SG1 = similar(:,11);
SG2 = similar(:,12);
SG3 = similar(:,13);

l4 = length(twosimSname);



%Find common genes in RANKL, salubrinal, and guanabenz treatments
%Then put into stimulatory and inhibitory groups
%Stimulatory = positive fold change in RANKL, negative fold
   change in salubrinal and guanabenz
%Inhibitory = negative fold change in RANKL, positive fold change
    in salubrinal and guanabenz
%added filtering condition where the absolute value of salubrinal
    and guanabenz expression cannot exceed control
for i3 = 1:l4,
    for i4 = 1:l1,
        if strcmp(twosimSname(i3), Rname(i4)),
            if ( twosimSFC(i3) < 0 && twosimGFC(i3) < 0 && RFC(
               i4) > 0 && (-1*twosimSFC(i3)) < RFC(i4) && (-1*
               twosimGFC(i3)) < RFC(i4)),
               threesim_neg = [threesim_neg ; twosimSname(i3)
                  twosimSFC(i3) twosimSpval(i3) twosimSlogFC(i3)
                   twosimGFC(i3) twosimGpval(i3) twosimGlogFC(i3
                  ) RFC(i4) Rpval(i4) RlogFC(i4) Rdef(i4) Racc(
```

```
                    i4) C1(i4) C2(i4) C3(i4) R1(i4) R2(i4) R3(i4)
                    SS1(i3) SS2(i3) SS3(i3) SG1(i3) SG2(i3) SG3(i3
                    )];
                elseif ( twosimSFC(i3) > 0 && twosimGFC(i3) > 0 &&
                   RFC(i4) < 0 && twosimSFC(i3) < (-1*RFC(i4)) &&
                   twosimGFC(i3) < (-1*RFC(i4))),
                   threesim_pos = [threesim_pos ; twosimSname(i3)
                    twosimSFC(i3) twosimSpval(i3) twosimSlogFC(i3)
                     twosimGFC(i3) twosimGpval(i3) twosimGlogFC(i3
                    ) RFC(i4) Rpval(i4) RlogFC(i4) Rdef(i4) Racc(
                    i4) C1(i4) C2(i4) C3(i4) R1(i4) R2(i4) R3(i4)
                    SS1(i3) SS2(i3) SS3(i3) SG1(i3) SG2(i3) SG3(i3
                    )];
                end
            end
        end
    end
end



%FOUR: Putting into Excel file, sheet 2 is final stimulatory
    group and sheet 4 is final inhibitory group.


header1 = {'Genes that are down-regulated in Salubrinal and
    Guanabenz compared to RANKL'};
header2 = {'Gene Symbol', 'Salubrinal FC', 'Pvalue S/R', '
    Salubrinal Log FC', 'Guanabenz FC', 'P value G/R', 'Guanabenz
    Log FC'};
xlswrite('Generestricted',header1,'Sheet1', 'A1')
xlswrite('Generestricted',header2,'Sheet1', 'A2')
```

```
xlswrite('Generestricted', similar_neg, 'Sheet1', 'A3')

header3 = {'Genes that are down-regulated in Salubrinal and
    Guanabenz compared to RANKL, but up-regulated in RANKL
    compared to Control'};
header4 = {'Gene Symbol', 'Salubrinal FC', 'Pvalue S/R', '
    Salubrinal Log FC', 'Guanabenz FC', 'P value G/R', 'Guanabenz
    Log FC', 'RANKL FC', 'P value R/C', 'RANKL Log FC', 'Gene
    definition', 'Accession number','C1', 'C2', 'C3','R1', 'R2', '
    R3','S1', 'S2', 'S3', 'G1', 'G2', 'G3'};
xlswrite('Generestricted',header3,'Sheet2', 'A1')
xlswrite('Generestricted',header4,'Sheet2', 'A2')
xlswrite('Generestricted', threesim_neg, 'Sheet2', 'A3')

header5 = {'Genes that are up-regulated in Salubrinal and
    Guanabenz compared to RANKL'};
header6 = {'Gene Symbol', 'Salubrinal FC', 'Pvalue S/R', '
    Salubrinal Log FC', 'Guanabenz FC', 'P value G/R', 'Guanabenz
    Log FC'};
xlswrite('Generestricted',header5,'Sheet3', 'A1')
xlswrite('Generestricted',header6,'Sheet3', 'A2')
xlswrite('Generestricted', similar_pos, 'Sheet3', 'A3')

header7 = {'Genes that are up-regulated in Salubrinal and
    Guanabenz compared to RANKL, but down-regulated in RANKL
    compared to Control'};
header8 = {'Gene Symbol', 'Salubrinal FC', 'Pvalue S/R', '
    Salubrinal Log FC', 'Guanabenz FC', 'P value G/R', 'Guanabenz
    Log FC', 'RANKL FC', 'P value R/C', 'RANKL Log FC', 'Gene
    definition', 'Accession number','C1', 'C2', 'C3','R1', 'R2', '
    R3','S1', 'S2', 'S3', 'G1', 'G2', 'G3'};
```

```
xlswrite('Generestricted',header7,'Sheet4', 'A1')
xlswrite('Generestricted',header8,'Sheet4', 'A2')
xlswrite('Generestricted', threesim_pos, 'Sheet4', 'A3')

'done'
```

A.2 Gene Distance and P-value

```
clear
clc

% Matlab inputs: gene names, signal values, and p-values - this
    also includes NFATc1
file = 'topdatarestrictednormalized.xlsx';

% ONE: importing data into individual arrays

%N = NFATc1-like, R = reciprocal
%C = control, R= RANKL, S= salubrinal, G = guanabenz

%stimulatory group
[numN stringR] = xlsread(file,1);
%gene names
Ngenename = stringR(2:end,1);
%gene fold change values
NSFC = numN(:,1);
NGFC = numN(:,2);
NRFC = numN(:,3);
%gene signal values
NS1 = numN(:,4);
NS2 = numN(:,5);
```

```
NS3 = numN(:,6);
NG1 = numN(:,7);
NG2 = numN(:,8);
NG3 = numN(:,9);
NR1 = numN(:,10);
NR2 = numN(:,11);
NR3 = numN(:,12);
NC1 = numN(:,13);
NC2 = numN(:,14);
NC3 = numN(:,15);
%gene p-values
PNS = numN(:,16);
PNG = numN(:,17);
PNR = numN(:,18);

%inhibitory group
[numR stringR] = xlsread(file,2);
%gene names
Rgenename = stringR(2:end,1);
%gene fold change values
RSFC = numR(:,1);
RGFC = numR(:,2);
RRFC = numR(:,3);
%gene signal values
RS1 = numR(:,4);
RS2 = numR(:,5);
RS3 = numR(:,6);
RG1 = numR(:,7);
RG2 = numR(:,8);
RG3 = numR(:,9);
RR1 = numR(:,10);
```

```
RR2 = numR(:,11);
RR3 = numR(:,12);
RC1 = numR(:,13);
RC2 = numR(:,14);
RC3 = numR(:,15);
%gene p-values
PRS = numR(:,16);
PRG = numR(:,17);
PRR = numR(:,18);

%putting into 1 array
NS = [NS1 NS2 NS3];
NG = [NG1 NG2 NG3];
NR = [NR1 NR2 NR3];
NC = [NC1 NC2 NC3];
%put into 1 array
RS = [RS1 RS2 RS3];
RG = [RG1 RG2 RG3];
RR = [RR1 RR2 RR3];
RC = [RC1 RC2 RC3];

%TWO: calculating mean signal values

%calculating mean signal values for stimulatory genes for each
    treatment category (N = NFATc1-like)
NSa = mean(NS,2);
NGa = mean(NG,2);
NRa = mean(NR,2);
NCa = mean(NC,2);
%calculating mean signal values for inhibitory genes for each
    treatment category (R = reciprocal)
```

```
RSa = mean(RS,2);
RGa = mean(RG,2);
RRa = mean(RR,2);
RCa = mean(RC,2);

%put into length
l1 = length (NSa);
l2 = length (RSa);

dN = zeros(l1,l1);
dR = zeros(l2,l2);
pNmean = zeros(1,l1);
pRmean = zeros(1,l2);
Ngenename2 = transpose(Ngenename);
Rgenename2 = transpose(Rgenename);

% THREE and FOUR: calculating each genes' distance and p-values
    using Pearson's correlation method and RMS p-value

Rsquarelike = zeros(1,l1);
Rlike = zeros(1,l1);
Rsquarerep = zeros(1,l2);
Rrep = zeros(1,l2);
NFS = NSa(1,1);
NFG = NGa(1,1);
NFR = NRa(1,1);
NFC = NCa(1,1);

%calculating distance and p-value for stimulatory group
for a = 1:l1,
    G = NSa(a) + NGa(a) + NRa(a) + NCa(a);
```

```
    N = NFS + NFG + NFR + NFC;
    Gsquare = (NSa(a)^2) + (NGa(a)^2) + (NRa(a)^2) +(NCa(a)^2);
    Nsquare = (NFS^2) + (NFG^2) + (NFR^2) + (NFC^2);
    GN = (NSa(a)*NFS) + (NGa(a)*NFG) + (NRa(a)*NFR) + (NCa(a)*NFC
        );
    Rsquarelike(a) = ((GN - ((G*N)/4)) / (sqrt((Gsquare - (((G)
        ^2)/4)) * (Nsquare - (((N)^2)/4))))) ^2;
    R = ((GN - ((G*N)/4)) / (sqrt((Gsquare - (((G)^2)/4)) * (
        Nsquare - (((N)^2)/4)))));
    Rlike(a) = (1-R)/2;
    pNm(a) = sqrt((((PNS(a)^2) + (PNG(a)^2) + (PNR(a)^2))/3));

end
%calculating distance and p-value for inhibitory group
for a = 1:12,
    G = RSa(a) + RGa(a) + RRa(a) + RCa(a);
    N = NFS + NFG + NFR + NFC;
    Gsquare = (RSa(a)^2) + (RGa(a)^2) + (RRa(a)^2) + (RCa(a)^2);
    Nsquare = (NFS^2) + (NFG^2) + (NFR^2) + (NFC^2);
    GN = (RSa(a)*NFS) + (RGa(a)*NFG) + (RRa(a)*NFR) + (RCa(a)*NFC
        );
    Rsquarerep(a) = ((GN - ((G*N)/4)) / (sqrt((Gsquare - (((G)^2)
        /4)) * (Nsquare - (((N)^2)/4))))) ^2;
    R = ((GN - ((G*N)/4)) / (sqrt((Gsquare - (((G)^2)/4)) * (
        Nsquare - (((N)^2)/4)))));
    Rrep(a) = (1-R)/2;
    pRm(a) = sqrt((((PRS(a)^2) + (PRG(a)^2) + (PRR(a)^2))/3));

end

%sorting in the order from closest to furthest distance
```

```
[lsort b] = sort(Rsquarelike,'descend');
Rlike = Rlike(b);
likename = Ngenename2(b);
likenamed = transpose(likename);
pNm = pNm(b);

[rsort c] = sort(Rsquarerep,'descend');
Rrep = Rrep(c);
repname = Rgenename2(c);
repnamed = transpose(repname);
pRm = pRm(c);

% FIVE: Put the names, distance, and p-value into an Excel file,
    sheet 1 is stimulatory group and sheet 2 is inhibitory group
header5 = {'Pearsons Distance table for top NFATc1-like genes'};
xlswrite('clusterrestnorm',header5,'Sheet1', 'A1')
xlswrite('clusterrestnorm',likename,'Sheet1', 'B2')
xlswrite('clusterrestnorm', likenamed, 'Sheet1', 'A3')
xlswrite('clusterrestnorm', lsort, 'Sheet1', 'B3')
xlswrite('clusterrestnorm', Rlike, 'Sheet1', 'B4')
xlswrite('clusterrestnorm', pNm, 'Sheet1', 'B5')

header6 = {'Pearsons Distance table for top NFATc1-reciprocal
    genes'};
xlswrite('clusterrestnorm',header6,'Sheet2', 'A1')
xlswrite('clusterrestnorm',repname,'Sheet2', 'B2')
xlswrite('clusterrestnorm', repnamed, 'Sheet2', 'A3')
xlswrite('clusterrestnorm', rsort, 'Sheet2', 'B3')
xlswrite('clusterrestnorm', Rrep, 'Sheet2', 'B4')
xlswrite('clusterrestnorm', pRm, 'Sheet2', 'B5')
```

```
'done'
```

B Prediction of Potential MicroRNA Regulators

The code for "MicroRNA Screening" and "MicroRNA Distance and P-value" are included in this category. The purpose of the "MicroRNA Screening" code is to filter the microarray data. This program takes the names, signal values, and p-values of 1625 microRNAs as input. The output is a list of filtered microRNAs. The procedure has four sections. First, the microarray data is imported, and each column was put into individual arrays. Second, the mean signal values and fold change values of each microRNA are calculated for each treatment category. Third, the microRNAs are filtered using filtering conditions based on signal value and p-value. Fourth, the output is written to an Excel file.

The purpose of the "MicroRNA Distance and P-value" code is to calculate the distance and p-value of each microRNA using Pearson's correlation method and RMS, respectively. The inputs are the names, signal values, and p-values of the filtered microRNAs from the results of "MicroRNA Screening". NFATc1 signal values are also used to calculate each microRNA's distance from NFATc1 expression pattern. The output of this program would be the calculated distance (d_i) and p-value (p_i) of each microRNA. The procedure includes four sections. First, the filtered microRNA data is imported, and each column was put into individual arrays. Second, the distance (d_i) of each microRNA is calculated using Pearson's correlation method. Third, the p-value of each microRNA is calculated using RMS. Fourth, the microRNA names, distance, and p-value are written into an Excel file ordered by distance.

B.1 MicroRNA Screening

```
clear, clc
%Matlab input: microRNA names, signal values, p-values
```

```
file = 'miRNArawdata.xlsx';


%ONE: importing data into individual arrays
[numR stringR] = xlsread(file,1);
%microRNA names
name = stringR(2:end,1);
%microRNA signal values C = control, R = RANKL, S = salubrinal, G
    = guanabenz
C1 = numR(:,1);
C2 = numR(:,2);
C3 = numR(:,3);
R1 = numR(:,4);
R2 = numR(:,5);
R3 = numR(:,6);
S1 = numR(:,7);
S2 = numR(:,8);
S3 = numR(:,9);
G1 = numR(:,10);
G2 = numR(:,11);
G3 = numR(:,12);
%microRNA p-values
PRC = numR(:,13);
PSR = numR(:,14);
PGR = numR(:,15);
%putting into one array
C = [C1 C2 C3];
R = [R1 R2 R3];
S = [S1 S2 S3];
G = [G1 G2 G3];


%TWO: calculating mean signal values and fold change values
```

```
%get the average of the signal values
Cmm = mean(C,2);
Rmm = mean(R,2);
Smm = mean(S,2);
Gmm = mean(G,2);
%ratio calculation (fold change)
ratRC = log2(Rmm./Cmm);
ratSR = log2(Smm./Rmm);
ratGR = log2(Gmm./Rmm);

%THREE: filtering based on signal mean and p-value

%also compiling to make sure they are the same length in each
    category list
%eliminating if signal mean is less than 500 and have poor p-
    value
a = find( (( PRC <= 0.05 )+( (Cmm >= 500) .* (Rmm >= 500) ) )>=1)
     ;
Cm = Cmm(a);
Cname = name(a);
C1 = C1(a);
C2 = C2(a);
C3 = C3(a);
Rm = Rmm(a);
Rname = name(a);
R1 = R1(a);
R2 = R2(a);
R3 = R3(a);
ratrc = ratRC(a);
c = find( (( PSR <= 0.05 )+( (Smm >= 500) .* (Rmm >= 500) ))>=1);
Sm = Smm(c);
```

```
Sname = name(c);
S1 = S1(c);
S2 = S2(c);
S3 = S3(c);
ratsr = ratSR(c);
d = find( (( PGR <= 0.05 )+( (Gmm >= 500) .* (Rmm >= 500) ))>=1);
Gm = Gmm(d);
Gname = name(d);
G1 = G1(d);
G2 = G2(d);
G3 = G3(d);
ratgr = ratGR(d);

%find the matches, make them the same length at the end
l1 = length(Cname);
l2 = length(Rname);
l3 = length(Sname);
l4 = length(Gname);
sim = [];
dim = [];
s = [];
for i1 = 1:l1,
    for i2 = 1:l2,
        if strcmp(Cname(i1),Rname(i2)),
            sim = [sim; Cname(i1) Cm(i1) C1(i1) C2(i1) C3(i1) Rm(
                i2) R1(i2) R2(i2) R3(i2) ratrc(i2)];
        end
    end
end
name1 = sim(:,1);
sCm = sim(:,2);
```

```
sC1 = sim(:,3);
sC2 = sim(:,4);
sC3 = sim(:,5);
sRm = sim(:,6);
sR1 = sim(:,7);
sR2 = sim(:,8);
sR3 = sim(:,9);
sratrc = sim(:,10);
for i1 = 1:l3,
    for i2 = 1:l4,
        if strcmp(Sname(i1),Gname(i2)),
            dim = [dim; Sname(i1) Sm(i1) S1(i1) S2(i1) S3(i1) Gm(
                i2) G1(i2) G2(i2) G3(i2) ratsr(i1) ratgr(i2)];
        end
    end
end
name2 = dim(:,1);
dSm = dim(:,2);
dS1 = dim(:,3);
dS2 = dim(:,4);
dS3 = dim(:,5);
dGm = dim(:,6);
dG1 = dim(:,7);
dG2 = dim(:,8);
dG3 = dim(:,9);
dratsr = dim(:,10);
dratgr = dim(:,11);
l5 = length(name1);
l6 = length(name2);
for i1 = 1:l5,
    for i2 = 1:l6,
```

```
        if strcmp(name1(i1),name2(i2)),
            s = [s; name1(i1) sCm(i1) sC1(i1) sC2(i1) sC3(i1) sRm
                (i1) sR1(i1) sR2(i1) sR3(i1) dSm(i2) dS1(i2) dS2(
                i2) dS3(i2) dGm(i2) dG1(i2) dG2(i2) dG3(i2) sratrc
                (i1) dratsr(i2) dratgr(i2)];
        end
    end
end
%new matched data and signal above 500
name = s(:,1);
Cm = cell2mat(s(:,2));
C1 = s(:,3);
C2 = s(:,4);
C3 = s(:,5);
Rm = cell2mat(s(:,6));
R1 = s(:,7);
R2 = s(:,8);
R3 = s(:,9);
Sm = cell2mat(s(:,10));
S1 = s(:,11);
S2 = s(:,12);
S3 = s(:,13);
Gm = cell2mat(s(:,14));
G1 = s(:,15);
G2 = s(:,16);
G3 = s(:,17);
RoC = Rm./Cm;
SoR = Sm./Rm;
GoR = Gm./Rm;
```

```
%FOUR: putting output into an Excel file

header2 = {'microRNA names', 'Control Mean', 'C1', 'C2','C3', '
    Rankl Mean', 'R1', 'R2', 'R3', 'Salubrinal Mean', 'S1', 'S2',
    'S3', 'Guanabenz Mean', 'G1', 'G2', 'G3', 'FC-RC', 'FC-SR', '
    FC-GR'};
xlswrite('miRNAforclusternewrestr',header2,'Sheet3', 'A2')
xlswrite('miRNAforclusternewrestr', s, 'Sheet3', 'A3')



'done'
```

B.2 MicroRNA Distance and P-value

```
clear
clc
%Matlab input: filtered microRNA names, signal values, p-values (
    also include NFATc1's)
file = 'clustermiRNArestr.xls';

%ONE: importing data into individual arrays
[numN stringR] = xlsread(file,1);
%microRNA names
Ngenename = stringR(2:end,1);
%microRNA signal values and p-values. C = control, R= RANKL, S=
    salubrinal, G= guanabenz
Cm = numN(:,1);
C1 = numN(:,2);
C2 = numN(:,3);
C3 = numN(:,4);
Rm = numN(:,5);
```

```
R1 = numN(:,6);
R2 = numN(:,7);
R3 = numN(:,8);
PRC = numN(:,9);
Sm = numN(:,10);
S1 = numN(:,11);
S2 = numN(:,12);
S3 = numN(:,13);
PSR = numN(:,14);
Gm = numN(:,15);
G1 = numN(:,16);
G2 = numN(:,17);
G3 = numN(:,18);
PGR = numN(:,19);

%TWO and THREE: Pearson's Correlation based on NFATc1 expression
    and RMS p-values calculation

NFS = Sm(1,1);
NFG = Gm(1,1);
NFR = Rm(1,1);
NFC = Cm(1,1);
l1 = length(Cm);
Rsquare = zeros(1,l1);
Rlike = zeros(1,l1);

for a = 1:l1,
    G = Sm(a) + Gm(a) + Rm(a) + Cm(a);
    N = NFS + NFG + NFR + NFC;
    Gsquare = (Sm(a)^2) + (Gm(a)^2) + (Rm(a)^2) +(Cm(a)^2);
    Nsquare = (NFS^2) + (NFG^2) + (NFR^2) + (NFC^2);
```

```
    GN = (Sm(a)*NFS) + (Gm(a)*NFG) + (Rm(a)*NFR) + (Cm(a)*NFC);
    Rsquarelike(a) = ((GN - ((G*N)/4)) / (sqrt((Gsquare - (((G)
        ^2)/4)) * (Nsquare - (((N)^2)/4))))) ^2;
    R = ((GN - ((G*N)/4)) / (sqrt((Gsquare - (((G)^2)/4)) * (
        Nsquare - (((N)^2)/4)))));
    Rlike(a) = (1-R)/2;
    pNm(a) = sqrt((((PRC(a)^2) + (PSR(a)^2) + (PGR(a)^2))/3));

end
%sorting from closest to furthest
Ngenename2 = transpose(Ngenename);
[lsort b] = sort(Rsquarelike,'descend');
Rlike = Rlike(b);
likename = Ngenename2(b);
likenamed = transpose(likename);
pNm = pNm(b);

% FOUR: putting output into an Excel file

header5 = {'Pearsons Distance table'};
xlswrite('PNnorest',header5,'Sheet1', 'A1')
xlswrite('PNnorest',likename,'Sheet1', 'B2')
xlswrite('PNnorest', likenamed, 'Sheet1', 'A3')
xlswrite('PNnorest', lsort, 'Sheet1', 'B3')
xlswrite('PNnorest', Rlike, 'Sheet1', 'B4')
xlswrite('PNnorest', pNm, 'Sheet1', 'B5')

'done'
```